Available online at www.sciencedirect.com
SCIENCE DIRECT®
Physica D 192 (2004) 161–186
PHYSICA D
www.elsevier.com/locate/physd

Uniqueness of solutions for constrained Elastica

A. Pocheau*, B. Roman

IRPHE, CNRS, Universités Aix-Marseille I & II, Technopole de Château-Gombert, 49 Rue Joliot-Curie, BP 146, F-13384 Marseille Cedex 13, France

Received 10 December 2001; received in revised form 30 April 2003; accepted 22 December 2003
Communicated by L. Kramer

Abstract

We address the number of solutions in constrained Elastica, i.e. the number of forms and tensions possibly adopted by steady rods or sheets enclosed in a prescribed box. Our main result refers to sheets making contact with the compressing plates at their extremities only. For these so-called folds, we provide the first demonstration of uniqueness of solution. This result is obtained by combining direct methods that are focused on definite families of solutions and global methods that address the structure of the set of solutions in the parameter space. While the first methods are specific to Elastica, the latter are not and may be applied to other kinds of systems. We then address the origins of the multiplicity of solutions in more general configurations and find two of them: geometrical non-linearity; freedom in the distribution of the length of flat contacts. The former gives rise to two free-standing fold solutions beyond buckling; the latter yields multiple buckling thresholds and thus multiple elastic responses to compression. Altogether, these results improve the non-local analysis of Elastica and clarify the reasons for unique or multiple buckling thresholds in constrained configurations. Moreover, fold uniqueness appears very useful for saving computational times in the numerical quest for solutions, for detecting parasitic solutions in simulations, for establishing the robustness of the Euler's model and for clarifying the role of friction. On a more general ground, our study provides non-local methods for determining the conditions for bifurcation in constrained systems involving a free energy.

PACS: 05.45.−a; 46.25.−y; 47.54.+r; 62.20.−x

Keywords: Uniqueness; Buckling; Plates; Non-linear eigenvalues; Elastic materials

1. Introduction

The Elastica denotes the model introduced by Euler to describe the equilibrium forms adopted by rods bent by imposed elastic constraints [1]. Since then it has been extended to systems involving no stretching: thin plates or sheets in the case where they display parallel folds [2], loaded arches [3,4] and the plane loops formed by rods that are closed on themselves [5]. The main advantage of the Euler's model is to accurately provide the forms, the tensions and the buckling thresholds of many elastic systems submitted to *prescribed* elastic *constraints*. In many situations, however [6–14], boundaries confine rods or sheets to a *prescribed volume* in which they have to

* Corresponding author. Tel.: +33-4-9613-9753; fax: +33-4-9163-9709.
E-mail address: alain.pocheau@irphe.univ-mrs.fr (A. Pocheau).

0167-2789/$ – see front matter © 2004 Elsevier B.V. All rights reserved.
doi:10.1016/j.physd.2003.12.013

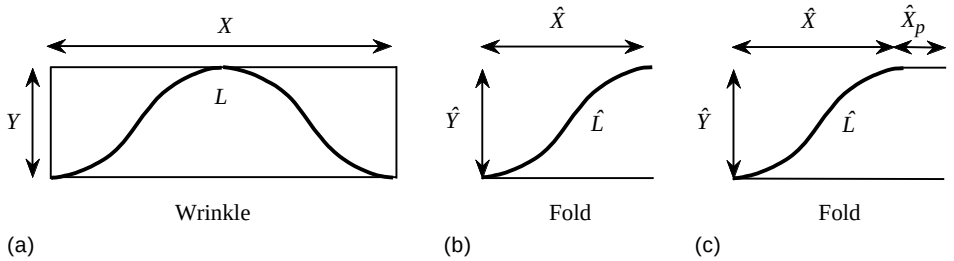

Fig. 1. (a) Sketch of a sheet of length L enclosed in a rectangular box of size X and Y. Here the sheet returns to the bottom plate after having touched the upper plate. This configuration is called *wrinkle*. (b) Sketch of a sheet part involving no other contact points than its extremities. This configuration is called a *fold*. Fold lengths are labeled $\hat{X}$, $\hat{Y}$, $\hat{L}$. (c) Same as in (b) in the case where the fold involves an extended part with length $\hat{X}_p$. As flat parts do not push on the supporting plate, they can be considered as involving contact only at their extremities too. Notice that all folds correspond to isolated mechanical systems in between their contact points with the compressing plates.

lie (Figs. 3–6). Then, the variables that are imposed are no longer elastic but geometric. This means that elastic constraints have now to adjust themselves so as to enable rods or sheets to fit the geometrical constraints. This configuration corresponds to the so-called constrained Elastica.

A natural issue in constrained Elastica consists in determining the number of possible solutions fitting prescribed geometrical bounds: can *multiple* forms be found for rods of given length L enclosed in a rectangular box of width X and height Y (Fig. 1a) or does *uniqueness* prevails? This question is important in practice since different branches of solution correspond to different mechanical responses, that can be chosen either for stocking maximum amount of energy or for providing an easier compression and smaller forces on the compressing device. In addition, as different branches undergo buckling at different loading, multiplicity of solutions provides the opportunity of monitoring the occurrence of bifurcation in the system. On the opposite, in case of uniqueness, the elastic constraints would simply appear as prescribed by geometrical bounds, despite the non-linearities brought about by the form of the compressed system. This, in particular, could be used to save computational time in the quest for solutions by path following method or by scan in parameter space [10,11].

In the following we will prove that, for any given geometric conditions, there exists at most one *unique* equilibrium configuration for a sheet starting from one plate and ending at the other plate *without* involving *any* other contact point in between (Fig. 1b). We shall call this property "fold uniqueness". Although it can be suspected from experimental [6–9,14,15] and computational [10,11,16–18] studies, it has to our knowledge neither been proved nor addressed theoretically. Once established, it will be used to understand more general configurations, including asymmetry (Fig. 6) and multiple contact points with the compressing box (Figs. 1a and 2–5). In these later cases, multiplicity of solutions has been largely observed in both stable or unstable states [1,6–11,14–18] and has been documented by

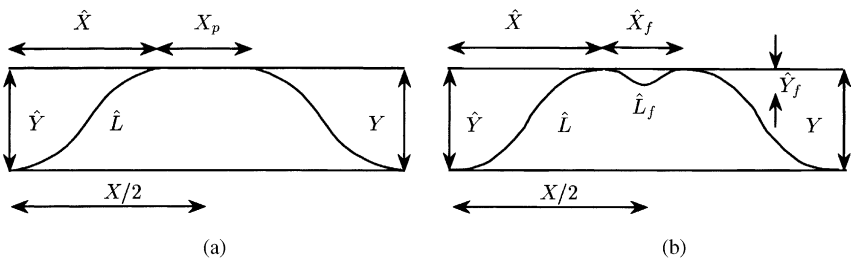

Fig. 2. Definitions of lengths for a sheet involving: (a) a flat contact part; (b) a free-standing fold.

computational approach including direct integration of the Euler's equation, path following method and extensive scan of parameter space [10,11]. Here, our goal will not be to address the very complex structure of this space of solutions but, instead, to classify the different sources of multiplicity of solutions and emphasize some of their properties. In addition, fold uniqueness will be used to examine and clarify the role of friction in this system.

Beyond constrained Elastica, the present problem of uniqueness of solutions in a system modeled by an ODE with global constraints refers to the question of the selection of non-linear eigenvalues by integral conditions: here, the selection of the integral (p, q) of the elastic constraints $(\sigma_{xx}, \sigma_{yy})$ over the system thickness by the geometric conditions (X, Y, L). This issue, which stands as a canonical one in applied mathematics, is analogous to addressing stigmatism in classical optics (how many rays may connect two points depending on the optical index field?) or to determining the spectrum of non-linear eigenvalues in propagating systems (how many constant velocities may display a propagating front for given external conditions?). Its main difficulty is that different solutions may stand far from each other in phase space. Accordingly, all the methods that restrict attention to a sub-part of the phase space or that use approximate equations are inappropriate for concluding about uniqueness. This includes methods based on linear analysis [17], on iterative search within formal solutions [19] or on shooting procedures [4,19]. In addition, methods based on a global scanning but with finite accuracy cannot be considered as a proof, first because limited accuracy may prevent the detection of multiplicity and, second, because discretization is known to sometimes generate spurious solutions [10,11]. Non-local theoretical methods, valid on the whole phase space, are thus required to address uniqueness.

Fold uniqueness for given geometrical bounds (X, Y, L) will be proved here by joining together complementing methods. "Direct methods" will be used to demonstrate uniqueness on *particular* curves of the parameter space; "global methods", based on integral properties of the system, will be used to extend this property to the *whole* parameter space. Altogether, they provide the first demonstration that there exists a *single* way of enclosing an elastic sheet in a rectangular box without allowing other contact points than the sheet extremities. On the other hand, global methods appear of particular interest, because they may apply to similar problems in other dynamical systems involving a free energy. One of them extends uniqueness in parameter space from a closed boundary to the *enclosed* parameter domain. Another method, deduced from the analysis of the conditions for bifurcations of branches of solutions shows that the property of uniqueness, i.e. the absence of bifurcation, naturally *propagates* itself in the parameter space following a definite *flow*.

The paper is organized as follows. Section 2 introduces constrained Elastica. Section 3 reports integral properties of constrained Elastica that will prove to be useful for addressing uniqueness. The derivation of uniqueness when the number of contact points is minimum is given in Section 4. It includes five steps that progressively extend the property of uniqueness to the whole space of geometrical constraints: the first three steps demonstrate uniqueness on closed lines of this space; the fourth step extends this result to the domain enclosed in this line; the fifth step generalizes uniqueness to the current tube generated by advection of this domain by a definite flow. Section 5 examines how this property can nevertheless give rise to a multiplicity of solutions for a larger number of contact points. It then addresses other important consequences of the property of uniqueness as regards to the experimental features of a compressed sheet. A conclusion about this work is given in Section 6.

2. Constrained Elastica

We consider a sheet (resp. a rod) of length L, width l, that is forced to lie in a parallelepiped (resp. rectangular) box of width X, $X < L$, and height Y and which is submitted to clamping boundary conditions at both ends (Fig. 1a). Our main issue will be to address the number of steady states that are available in this constrained situation and, especially, to demonstrate uniqueness in the so-called fold configuration (Fig. 1b). Although this work is theoretical,

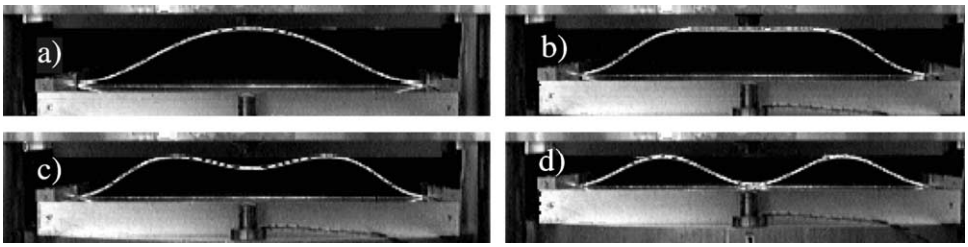

Fig. 3. Transition from one to two wrinkles: side view of polycarbonate sheet, $E \approx 2\,\mathrm{GPa}$, $X = 220\,\mathrm{mm}$, $L = 233\,\mathrm{mm}$, $l = 101\,\mathrm{mm}$, $h = 1\,\mathrm{mm}$, $R = L/X - 1 = 0.06$. *Steady* forms: (a) line contact: $Y = Y_1$, (b) planar contact: $Y_\mathrm{p} > Y > Y_b$, (c) post-buckling with free-standing fold: $Y_b > Y > Y_2$, and (d) two wrinkles similar to the one of (a): $Y = Y_2$.

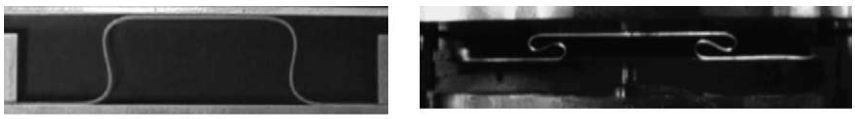

Fig. 4. Large relative surface excess $R = L/X - 1$: (a) $0.8 > R > 0.3$. *S*-like form involving an upper fold part overhanging the lower fold part. The flat part will eventually buckle at higher compression. (b) $R > 0.8$. Mushroom-like form. It involves a flat part on which tension is too small to ever induce buckling as the height Y is reduced.

it is worth illustrating it experimentally below by showing examples of the various forms displayed by compressed sheets. Of course, these observations cannot pretend to be neither exhaustive nor free of disturbances. Accordingly, they can only provide counter-examples of uniqueness if several solutions are evidenced. In particular, they cannot be considered as an actual proof of uniqueness, even if only a single solution could be observed. We shall follow their report by a short description of the Euler's model.

2.1. Constrained shapes

Possible constrained shapes are illustrated by the snapshots obtained in an experimental set-up in which box height Y is reduced at fixed length constraints (X, L) [14,18]. Notice that, as the sheet length L is taken larger than the box size X, the sheet is initially buckled before compression. Then, reducing Y makes the sheet adopt various shapes and various tensions, so as to adapt compression. The first shapes observed on the compression routes involve a constrained arch (Fig. 3a) with possibly a flat part (Fig. 3b). Depending on the ratio L/X, further height reduction yields the flat part to buckle (Fig. 3c) or not (Fig. 4a), hence generating a suspended arch in the former case (Fig. 3c) and folds overhanging themselves in the latter case (Fig. 4). Notice that these forms are symmetric. However, external perturbations can yield additional steady states that are asymmetric (Fig. 6).

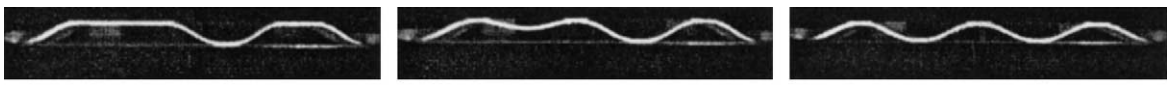

Fig. 5. Buckling of a configuration involving multiple wrinkles: side view of polycarbonate sheet, $E \approx 2\,\mathrm{GPa}$, $X = 220\,\mathrm{mm}$, $L = 233\,\mathrm{mm}$, $l = 101\,\mathrm{mm}$, $h = 1\,\mathrm{mm}$, $R = L/X - 1 = 0.06$. *Steady* forms: (a) planar contact: $Y_2 > Y > Y_b$, (b) post-buckling with free-standing fold: $Y_b > Y > Y_3$, and (c) an additional wrinkle is formed: $Y = Y_3$.

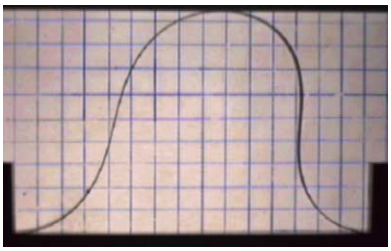

Fig. 6. Asymmetric steady states. These states cannot be naturally obtained from unloaded states. They actually require finite amplitude perturbation.

When reducing the box height further, the buckling history described in Fig. 3 resumes. However, among the various flat parts that are displayed, only a single one, the largest, undergoes buckling (Fig. 5a). One then obtains multiple wrinkles (Fig. 5c), sometimes showing flat parts (Fig. 5a) or a single suspended part (Fig. 5b).

In the sequel, we shall call "wrinkle" a sheet part going from one compressing plate to the other and *returning* (Figs. 2a and 3a). However, it will appear important to consider those parts of the sheet that may be considered as an *isolated* mechanical system. They correspond to sheet parts in between two consecutive contact points with the compressing plates. We shall call them a "fold".

Examples of folds are given by half the sheet of Fig. 3a or by the left part of sheets of Fig. 3b–d, until they touch the upper plate. Their lengths will be denoted as $(\hat{X}, \hat{Y}, \hat{L})$ (Figs. 1 and 2a). Folds can also correspond to the extended flat parts of Figs. 3b, 4 and 5a. Their lengths will then be labeled X_{p} on a sheet (Fig. 2a) and $\hat{X}_{\mathrm{p}}$ on a fold (Fig. 1b). The last possible kind of folds is finally provided by the "suspended" sheet parts generated by buckling of flat contact parts (Figs. 2b, 3c and 5b). They correspond to folds that connect the same compressing plate. They will be called hereafter free-standing fold and their lengths will be denoted $(\hat{X}_{\mathrm{f}}, \hat{Y}_{\mathrm{f}}, \hat{L}_{\mathrm{f}})$ (Fig. 2b). Accordingly, in the remaining of this study, the labels $(^{\wedge}, _{\mathrm{p},\mathrm{f}})$ will simply refer to a fold, a planar part and a free-standing part.

When reducing the allowable height Y, the different routes followed by the system are parameterized by the remaining constraints (X, L) or, because of the absence of intrinsic length in the Elastica, by their ratio L/X. In the following, we shall prefer introducing an equivalent parameter, the *relative* excess R of the sheet length L (or the sheet surface $L \times l$) as compared to the plate length X (or the plate surface $X \times l$): $R = L/X - 1$.

2.2. Elastica

The Elastica model by Euler [1] describes the mechanical equilibrium of a rod, $l \ll L$, undergoing an external force *only* at its ends. It is thus a priori restricted to folds but may be iterated to describe a succession of folds, i.e. a sheet. It is formulated in differential form by expressing the equilibrium of any elementary rod part located in between curvilinear abscissa s and $s + \mathrm{d}s$. It has later been extended to infinitely large plates, $l \gg L$, involving parallel folds only [2,20].

Owing to linear elasticity, the moment applied at one end of an elementary part of a fold is proportional to its curvature $1/\rho$: $M = EI/\rho$. Here, E is the Young's modulus and $I(h, l)$ a coefficient, the moment of inertia of the sheet cross-section, which depends on its geometry, i.e. on its width l and thickness h. An expression for $I(h, l)$ can be explicitly derived in the two opposite limits of a rod $l \ll \hat{L}$, and of an infinite sheet $\hat{L} \ll l$, both with infinitely thin thickness $h \ll l$, $h \ll \hat{L}$ [2,20]. Since elasticity involves no characteristic scale in these regimes, the dependence of coefficient I on either lengths h and l is scale-invariant. It thus expresses with power laws: $I = \alpha l h^3/12$, where the prefactor α depends on the asymptotic limit: $\alpha = 1$ for rods; $\alpha = (1-\nu^2)^{-1}$ for infinite sheets [2,20], ν denoting the

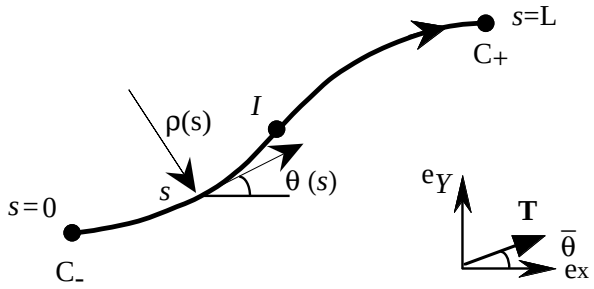

Fig. 7. Sketch of the geometrical representation of folds in Elastica. $\theta(s)$ denotes the angle of the fold tangent with the X-axis, $\rho(s)$ the fold curvature radius at curvilinear abscissa s and $\mathbf{T}$ the fold tension. The angle between the constant tension $\mathbf{T}$ and the X-axis is labeled $\bar{\theta}$. C_-, C_+ are the contact points of the sheet with the compressing plate and I its inflexion point.

Poisson's ratio. The origin of the differences in the values of α lies in the coupling on transverse directions between stresses and deformations, as expressed by the coupling coefficient ν.

Consider now the curve $\mathcal{C}$ given by the projection of the sheet on the direction of the fold axis. We focus attention on an elementary sheet part located in between s and $s + \mathrm{d}s$ (Fig. 7). It is submitted to a tension $\mathbf{T}(s)$ whose components are labeled $p(s)$, $q(s)$. We note $\theta(s) \equiv \theta_s$ the angle between the tangent to curve $\mathcal{C}$ at location s and the fixed direction $\mathbf{e}_X$. Moment equilibrium of the sheet part yields

$$EI\frac{\mathrm{d}^2\theta}{\mathrm{d}s^2} = -p(s)\sin\theta + q(s)\cos\theta. \tag{1}$$

In addition, force equilibrium over the sheet part implies that tension $\mathbf{T} = (p, q)$ is *constant* along the sheet:

$$p(s) = p, \qquad q(s) = q. \tag{2}$$

Altogether, Eqs. (1) and (2) provide the Euler's equation for the so-called Elastica problem. It undergoes boundary conditions which, in the present case, are clamping conditions:

$$\theta(0) = \theta_0 = 0, \qquad \theta(\hat{L}) = \theta_{\hat{L}} = 0. \tag{3}$$

Interestingly, denoting the derivative $\mathrm{d}\theta/\mathrm{d}s$ by $\dot{\theta}$, the Euler's equation may be recovered by minimizing the elastic curvature energy $E_c = \int_0^{\hat{L}} (\dot{\theta}^2/2)\,\mathrm{d}s$ of a fold at fixed initial and final angles $(\theta_0, \theta_{\hat{L}})$ and under the geometrical constraints $\hat{X} = \int_0^{\hat{L}} \cos(\theta)\,\mathrm{d}s$, $\hat{Y} = \int_0^{\hat{L}} \sin(\theta)\,\mathrm{d}s$. Introducing Lagrange multipliers (p, q), this comes down to minimizing the functional $\mathcal{A}[p, q; \theta(s)] = E_c + p\hat{X} + q\hat{Y}$ with respect to the sheet form $\theta(s)$, at *fixed* initial and final angles $(\theta_0, \theta_{\hat{L}})$: $(\delta\mathcal{A}/\delta\theta)|_{\theta_0,\theta_{\hat{L}}} = 0$.

Formal solutions of the Elastica correspond to the elliptic integrals (A.4) that implicitly relate the fold lengths $(\hat{X}, \hat{Y}, \hat{L})$ to the tension components (p, q) and to the angle θ_I of the tangent of the sheet at the fold inflexion point I (Fig. 7) (see Appendix A.1).

3. Integral properties of constrained Elastica

We restrict attention here to the *isolated* system on which the Elastica is defined: the *fold* (Fig. 1b and c). After having recalled some integral properties of constrained Elastica, we derive from them some relationships that will prove to be useful for demonstrating fold uniqueness in Section 4.

The interest of integral relationships here comes from the following problem. Once the fold tension (p, q) is given, the fold geometry is univocally prescribed as a solution of an ordinary differential equation (1) with boundary conditions $\theta_0 = 0$, $\dot{\theta}_0 = (p\hat{Y} - q\hat{X})/2$ (see relation (9)). Accordingly, solving for constrained Elastica then reduces to determining the values (p, q) for which the Elastica solution succeeds in fitting within the geometrical bounds. Solving for this kind of *non-linear eigenvalue* problems is usually a hard task, unless there exist integral relationships capable of connecting initial and final conditions [21]. In particular, here, using the formal solutions (A.4) of the problem proves to be a inadequate framework for pointing out the relevant properties of the Elastica. The reason is that most of these properties come from non-local features of the system which, although formally included in these exact solutions, are not explicitly exhibited. In other words, the differential equation (1) corresponds to a local analysis that proves to be unsuitable to fully address the global properties of the system. Conversely, using integral relationships makes one go up to a non-local ground which is more suited to the physics of the present system. In particular, expressing from these integral relationships the compatibility between initial and final conditions often yields an analytic determination of non-linear eigenvalues and, finally, of the solution [21].

In the following, we shall mostly try to follow this track by determining from the Elastica's properties some relevant integral relationships to be applied in the next section. These will follow from the existence of an underlying variational principle (4), a Hamiltonian (6), a conserved flux along the sheets (6) and an internal energy (5). To simplify the notations, we shall take hereafter $EI \equiv 1$, thanks to a change of units.

3.1. Action, external work and energy conservation

In Section 2.2, we have recalled that the Euler's equation can be derived from the minimization of a functional $\mathcal{A}[p, q; \theta(s)] = E_c + p\hat{X} + q\hat{Y}$ with respect to sheet form $\theta(s)$ at fixed initial and final angles $(\theta_0, \theta_{\hat{L}})$. Interestingly, we note that this variational property yields energy conservation for the system made by the compressed sheet and the operator providing the compression. This can be shown by considering a *steady* state $\mathcal{S}$ referring to parameters $(\hat{X}, \hat{Y}, \hat{L}, p, q)$ and by applying an elementary variation of the box sizes $\hat{X}$, $\hat{Y}$. One obtains another *steady* state $\mathcal{S}'$ referring to the parameters $(\hat{X}', \hat{Y}', \hat{L}, p', q')$ corresponding to $\hat{X}' = \hat{X} + \mathrm{d}\hat{X}$, $\hat{Y}' = \hat{Y} + \mathrm{d}\hat{Y}$. The fact that $\mathcal{S}$ is a *solution* of the Euler's equations can now be expressed by applying, in its vicinity, the steadiness of the action $\mathcal{A}[p, q; \theta(s)]$ with respect to form variations $\mathrm{d}\theta(s)$ with $\mathrm{d}\theta_0 = \mathrm{d}\theta_{\hat{L}} = 0$. This comes down to stating that the variation of the action $\mathrm{d}\mathcal{A}$ when going from the form $\mathcal{S}$ to the form $\mathcal{S}'$ at *fixed* multipliers (p, q) is of higher order than the state difference $(\mathrm{d}\hat{X}, \mathrm{d}\hat{Y})$: $\mathrm{d}\mathcal{A} = \mathrm{o}(\mathrm{d}\hat{X}, \mathrm{d}\hat{Y})$. One obtains in this way:

$$\mathrm{d}\mathcal{A} = \mathrm{d}E_c + p\,\mathrm{d}\hat{X} + q\,\mathrm{d}\hat{Y} = \mathrm{o}(\mathrm{d}\hat{X}, \mathrm{d}\hat{Y}). \tag{4}$$

Calling $\delta W = -p\,\mathrm{d}\hat{X} - q\,\mathrm{d}\hat{Y}$ the work done by the operator during compressions $\mathrm{d}\hat{X}$, $\mathrm{d}\hat{Y}$, relation (4) yields

$$\mathrm{d}E_c = -p\,\mathrm{d}\hat{X} - q\,\mathrm{d}\hat{Y} = \delta W \tag{5}$$

at first order in $(\mathrm{d}\hat{X}, \mathrm{d}\hat{Y})$. As the steady states $\mathcal{S}, \mathcal{S}'$ involve no kinetic energy, E_c represents the internal energy of the box. Accordingly, the principle of least action *implies* here energy conservation (5) for the *non-isolated* compressed system under variations of the constraints $(\hat{X}, \hat{Y})$.

3.2. Autonomy and symmetry

Following relation (2), Euler's equation (1) is autonomous since its parameters, e.g. (p, q), are independent of curvilinear abscissa s. This implies an invariance of physical properties by any translation $s \to s + s_0$. Accordingly, there is no absolute origin in the mechanical system, so that the properties in form and tension of any part of the sheet are equivalent to those of any other. In particular, once tension $\mathbf{T} = (p, q)$ is given, initial conditions $(\theta, \dot{\theta})$ at

the beginning of a fold are entirely sufficient to determine it completely *without* reference to any other part of the sheet.

Following autonomy, the entire sheet can then be understood as *series* of branches connecting one plate to the other, any branch interacting with its *sole* neighbors at their common contact point *only*. This stands as a somewhat original property for an elastic system which, for instance, would be invalid if folds were no longer parallel. Especially, the initial problem of minimization of elastic energy under global constraints spectacularly reduces here to a small number of conditions at a few contact points. Also, once tension is given, the sheet can be analyzed piece by piece, despite the non-locality inherent to elasticity. This actually illustrates the fact that non-locality is entirely handled here in the couple of non-linear eigenvalues (p, q).

Euler's equation is invariant by reflection $s \to -s$. This means that folds can satisfy left–right symmetry, as observed in Figs. 3–6. That they must do results from the fact that, as the sheet is clamped between distant boundaries, it cannot reverse direction at a contact point. Accordingly, its curvatures in the vicinity of the extremities of each fold take opposite signs (Fig. 1b and c). This implies that it must vanish in between at an inflexion point $(\theta_\mathrm{I}, \dot\theta_\mathrm{I} = 0)$. At this point I, the Euler's equation develops the same solution forward $(s \to s)$ and backward $(s \to -s)$ since the initial condition and the equation are the same. This amounts to saying that the corresponding fold is symmetric with respect to the inflexion point I.

3.3. Integral invariant and curvature energy

The Elastica provides two integral invariants, a Hamiltonian $H(\theta, \dot\theta)$ and a net impulsion flux $B(\theta, \dot\theta)$ that satisfy $\mathrm{d}H/\mathrm{d}s = 0$ and $\mathrm{d}B/\mathrm{d}s = 0$.

$$H(\theta, \dot\theta) = \tfrac{1}{2}\dot\theta^2 - p\,\cos(\theta) - q\sin(\theta), \qquad B(\theta, \dot\theta) = \dot\theta + p\hat Y(s) - q\hat X(s) \tag{6}$$

with $\hat X(s) = \int_0^s \cos(\theta)\,\mathrm{d}\sigma$, $\hat Y(s) = \int_0^s \sin(\theta)\,\mathrm{d}\sigma$. They enable an easy determination of both the sheet curvature energy E_c and the impulsion $\dot\theta_0$ at the contact point.

Equating the Hamiltonian at the initial point $(\theta_0 = 0, \dot\theta_0)$ and at the inflexion point $(\theta_\mathrm{I}, \dot\theta_\mathrm{I} = 0)$, one obtains

$$H(0, \dot\theta_0) = \tfrac{1}{2}\dot\theta_0^2 - p = -p\,\cos(\theta_\mathrm{I}) - q\sin(\theta_\mathrm{I}) = H(\theta_\mathrm{I}, 0) \tag{7}$$

or

$$\dot\theta_0^2 = 4\sin(\tfrac{1}{2}\theta_\mathrm{I})[p\sin(\tfrac{1}{2}\theta_\mathrm{I}) - q\,\cos(\tfrac{1}{2}\theta_\mathrm{I})]. \tag{8}$$

Consider a steady fold connecting opposite plates (Figs. 1b and c and 7). Equating the net impulsion flux $B(\theta, \dot\theta)$ at the initial point $(\theta_0 = 0, \dot\theta_0)$ and at the inflexion point $(\theta_\mathrm{I}, \dot\theta_\mathrm{I} = 0)$ gives

$$B(0, \dot\theta_0) = \dot\theta_0 = \tfrac{1}{2}(p\hat Y - q\hat X) = B(\theta_\mathrm{I}, 0) \tag{9}$$

since, at the location s_I of the inflexion point, $\hat X(s_\mathrm{I}) = \hat X/2$ and $\hat Y(s_\mathrm{I}) = \hat Y/2$ owing to fold symmetry. On the other hand, the expression (6) of the Hamiltonian shows that the fold curvature energy reads

$$E_\mathrm{c} = \int_0^{\hat L} [H + p\,\cos(\theta) + q\sin(\theta)]\,\mathrm{d}s = \tfrac{1}{2}\hat L\dot\theta_0^2 - p(\hat L - \hat X) + q\hat Y \tag{10}$$

or, following (9):

$$E_\mathrm{c} = \tfrac{1}{8}(p\hat Y - q\hat X)^2\hat L - p(\hat L - \hat X) + q\hat Y. \tag{11}$$

Relation (11) is especially interesting since it directly links curvature energy to both geometrical constraints $(\hat X, \hat Y, \hat L)$ and elastic constraints (p, q) *without* explicit determination of the Elastica solution $\theta(s)$. In this respect, it stands as a thermodynamic relationship.

Consider now the *whole* sheet (Fig. 2) and assume, as usual, that plates do not bring moment to the sheet at the contact point by friction. Then, the initial "impulsion" $\dot\theta_0$ gets the same value on both sides of contact points. As p is constant along the sheet (2), this implies that the value (7) of the Hamiltonian remains the same all along the sheet: $\mathrm{d}H/\mathrm{d}s = 0$, $s \in [0, L]$. Integrating the density of curvature energy as in (10) then gives

- On flat parts ($\dot\theta_0 = 0$, $\hat L_\mathrm{p} = \hat X_\mathrm{p}$, $q = 0$):

$$E_\mathrm{c} = \tfrac{1}{2}\hat L_\mathrm{p}\dot\theta_0^2 - p(\hat L_\mathrm{p} - \hat X_\mathrm{p}) = 0 \tag{12}$$

  as expected here, since $\dot\theta(s) = 0$ and $\hat L_\mathrm{p} = \hat X_\mathrm{p}$ on flat parts.
- On free-standing folds ($q = 0$):

$$E_\mathrm{c} = \tfrac{1}{2}\hat L_\mathrm{f}\dot\theta_0^2 - p(\hat L_\mathrm{f} - \hat X_\mathrm{f}). \tag{13}$$

Adding the different curvature energies (10), (12) and (13) for a left–right symmetrical sheet (Fig. 2), one then obtains $L = 2\hat L + \hat L_\mathrm{p} + \hat L_\mathrm{f}$, $X = 2\hat X + \hat X_\mathrm{p} + \hat X_\mathrm{f}$, $Y = \hat Y$ and

$$E_\mathrm{c} = \tfrac{1}{2}L\dot\theta_0^2 - p(L - X) + qY. \tag{14}$$

This generalizes relation (10) to a whole sheet.

4. Uniqueness of folds

The purpose of this section is to demonstrate uniqueness of solution for constrained *folds*, i.e. for sheets involving a single contact with each of the compressing plates. This comes down to showing that there exists a single local minimum of the fold elastic energy (11). Surprisingly, no previous attempt to solve this problem has been reported in literature, to our knowledge. Accordingly, we find it valuable to analyze first the kind of strategy that might be relevant to address it.

As the global constraints for folds $(\hat X, \hat Y, \hat L)$ are formally related to the parameters $(p, q, \dot\theta_0)$ of the differential system by the relations (A.1) and (A.3) and the elliptic integrals (A.4), a possible strategy for addressing uniqueness might be to focus analysis on these formal relationships. However, this seems cumbersome, if not doomed to failure, in the general case of *incomplete* elliptic integrals, i.e. of formal solutions of the periodic orbit of the dynamical system (1) and (2) with *unprescribed* phase ϕ (A.3). One reason is the large number of degrees of freedom left out in the quest for alternate solutions, another is the technical complexity of elliptic integrals and a last reason is the possible existence of solutions *far* distant from each other in the parameter space. In view of these difficulties, we shall address fold uniqueness by combining several different tools:

- analysis of *complete* elliptic integrals (i.e. for $\phi = \pi/2$) (Sections 4.1 and 4.2);
- use of energy conservation (Section 4.3);
- analysis of one-parameter numerical solutions (Section 4.3);
- use of the variational character of the system (Section 4.4);
- analysis of the splitting of the branches of solutions (Section 4.5).

The combined use of different methods should not be seen here as a failure in simplifying the proof of fold uniqueness but as a necessity for solving a problem that, to date, has failed to be solved otherwise.

Following the absence of intrinsic length in the Elastica and the constancy of sheet length $\hat L$ during compression, we shall address the uniqueness problem in non-dimensional variables $(\hat X/\hat L, \hat Y/\hat L)$ or, equivalently, in the couple

of variables $(\hat{X}, \hat{Y})$ for a given length $\hat{L} \equiv 1$. Uniqueness will be shown by the following strategy:

- Scan of particular sets of solutions. We shall first focus attention on specific states for which the possible family of solutions involve few enough parameters to be easily scanned entirely. These will be the unloaded states ($q = 0$) (Section 4.1), the states involving flat contacts ($\dot{\theta}_0 = 0$) (Section 4.2) and the states for which $\hat{X} = 0$ (Section 4.3). These three lines of states will provide, in the constraint space $\mathcal{S} = \{(\hat{X}, \hat{Y}), \hat{L} \equiv 1\}$, a *closed* curve $\mathcal{L}$ on which uniqueness will be satisfied.
- Analysis of the constraint space. We shall extend uniqueness from the closed curve $\mathcal{L}$ to a domain by analyzing the properties of the system in the constraint space $\mathcal{S}$. Uniqueness will be shown to apply in the *interior* of curve $\mathcal{L}$ by use of the variational character of the system (Section 4.4) and in the *exterior* of $\mathcal{L}$ by analysis of the conditions of bifurcation of branches of solutions (Section 4.5).

These various methods will succeed in progressively extending the demonstration of uniqueness to the whole available constraint space for sheets compressed in a box.

4.1. Uniqueness for unloaded folds

Unloaded folds, i.e. $q = 0$, correspond either to the sheet prior to contact with the upper plate (Fig. 3a) or to a free-standing fold (Fig. 3c). Then, from (A.1) and (A.3), $\bar{\theta} = 0$ and $\phi = 0$, so that, following (A.4), fold lengths satisfy

$$\hat{L} = \frac{2}{\omega}F, \qquad \hat{X} = \frac{2}{\omega}(2E - F), \qquad \hat{Y} = \frac{2}{\omega}2k, \tag{15}$$

where $E \equiv E(\pi/2, k)$ and $F \equiv F(\pi/2, k)$ denote complete elliptic integrals and k, $\bar{\theta}$, ω and ϕ intermediate variables defined in (A.1) and (A.3).

From (15), the relative surface excess of folds, $\hat{R} = (\hat{L} - \hat{X})/\hat{X}$, appears as a function of k only: $\hat{R} \equiv \hat{R}(k)$. Fig. 8 shows that function $\hat{R}(\cdot)$ is *bijective*, so that $\hat{R}$ selects a *single* k: $k \equiv k(\hat{R})$. Following relation (15), ω is then univocally prescribed by $\hat{R}$ and $\hat{L}$. Accordingly, at given fold constraints $(\hat{X}, \hat{L})$, i.e. $(\hat{R}, \hat{L})$, there exists a *unique* choice of variables (k, ω) and thus a *unique* solution to this Elastica.

4.2. Uniqueness for folds involving flat contacts

We consider flat contacts: $\dot{\theta}_0 = 0$. We first address the states where flat contacts just appear, $\hat{X}_\mathrm{p} = 0$, before considering those where flat contacts are developed, $\hat{X}_\mathrm{p} > 0$. Regarding the birth states, we first show that they are *inevitably* encountered when compressing the sheets. We then prove the uniqueness of their occurrence on a

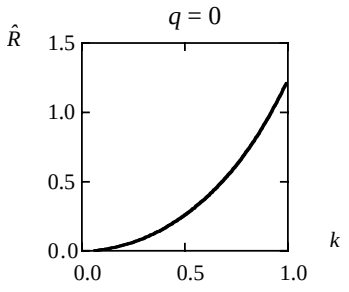

Fig. 8. Unloaded folds: $q = 0$. Evolution of the relative surface excess $\hat{R}$ with k.

compression route and we demonstrate that this corresponds to a *unique* sheet form. As a flat contact is a rest part of the dynamical system (1), we then easily reduce the case of extended flat contacts, $\hat{X}_p > 0$, to that of marginal flat contacts, $\hat{X}_p = 0$.

4.2.1. Necessary occurrence of flat contacts

Flat contacts are actually evidenced experimentally on compression routes (Figs. 3b, 4 and 5a). Is this observation specific to some control parameters or must flat contacts inevitably be encountered during height reduction?

To prove the *necessary* occurrence of flat contacts on *any* crushing route starting from the unloaded state, we first notice that, according to the expressions (A.4) of lengths in the line contact regime, the integral relationship (9) and the definitions (A.1) of variables $\bar{\theta}$ and ω, the initial impulsion $\dot{\theta}_0$ simply writes

$$\dot{\theta}_0 = 8\mathbf{E}^2 \frac{\hat{Y}\cos(\bar{\theta}) - \hat{X}\sin(\bar{\theta})}{[\hat{L} + \hat{X}\cos(\bar{\theta}) + \hat{Y}\sin(\bar{\theta})]^2}, \tag{16}$$

where $\mathbf{E}$ denotes the elliptic integral, $\mathbf{E} = E(\pi/2, k) - E(\phi, k)$ (A.2).

The important point for the sequel is that $\mathbf{E}$ is *bounded* in the line contact domain. This simply results from the following inequality:

$$\mathbf{E} = \int_{\phi}^{\pi/2} [1 - k^2 \sin^2(v)]^{1/2}\, \mathrm{d}v < \frac{\pi}{2} - \phi \tag{17}$$

and from the fact that the phase ϕ lies in between $\pi/2$ (e.g. $\hat{L} = 0$) and $-\pi/2$ (e.g. flat contact) on the line contact domain. Moreover, following uniqueness at $q = 0$, q must remain positive once compression has begun: $q > 0$. As, in our set-up, initial impulsion $\dot{\theta}_0$ is positive too, relation (9) implies that p is also positive: $p > 0$. Following (A.1), this means that both $\cos(\bar{\theta})$ and $\sin(\bar{\theta})$ are positive (i.e. $0 \le \bar{\theta} \le \pi/2$) so that, following (16) and (17), $\dot{\theta}_0$ is *bounded* in the line contact domain.

Consider now the line contact regime, $\dot{\theta}_0 > 0$, $\hat{X} = X$, $\hat{R} = R$ (Fig. 1) and decrease $\hat{Y}$. Following (9) and (10), the fold curvature energy satisfies: $2\hat{Y}E_c = \dot{\theta}_0\lambda + 2q\mu$ with $q \ge 0$, $\dot{\theta}_0 > 0$, $\lambda = \hat{Y}\hat{L}\dot{\theta}_0 - 4\hat{X}\hat{R}$ and $\mu = \hat{Y}^2 - \hat{X}^2\hat{R}$. As $\hat{Y}$ decreases, both μ and λ turn negative since $\dot{\theta}_0$ is bounded and $\hat{X}$, $\hat{R}$ are constant. As curvature energy E_c is defined *positive*, one must therefore necessarily escape this regime at some height $\hat{Y}_p$ by entering the flat contact domain $\dot{\theta}_0 = 0$, where $\hat{X}$, $\hat{R}$ are no longer fixed. Moreover, as this must occur for still positive μ, the transition height $\hat{Y}_p$ is *bounded* by below: $\hat{Y}_p > \hat{X}\hat{R}^{1/2}$.

4.2.2. Uniqueness of the occurrence of flat contact

Reducing $\hat{Y}$, a flat contact must thus appear. Assume now that different branches of solutions could have been followed. Each would yield a flat contact at some specific height $\hat{Y}_p(\hat{X}, \hat{L})$. Could this height depend on the branch of solution?

When a flat contact has just appeared, its length is by continuity zero, $\hat{X}_p = 0$, so that the relative surface excess of a fold $\hat{R}$ takes a definite value: $\hat{R} = R$ (Fig. 2a). On the other hand, in the flat contact domain, both variables $\hat{R}$ and $\hat{\xi} = \hat{Y}/(\hat{L} - \hat{X})$ stand as functions of the *sole* variable k (A.7). They are therefore directly related one to the other (A.7): $\hat{R} \equiv \hat{R}(\hat{\xi})$. However, Fig. 9a shows that the relationship $\hat{R}(\cdot)$ is bijective at least in the domain of flat contact occurrence. This means that, for given $(\hat{X}, \hat{L})$ and whatever the branch of solution followed from the unloaded state, flat contacts can only appear at a *single* $\hat{\xi} \equiv \hat{\xi}_p$, such that $\hat{R}(\hat{\xi}_p) = R$. This corresponds to a *single* height, $\hat{Y}_p$, given by $\hat{Y}_p = \hat{\xi}_p(\hat{L} - \hat{X})$. A corollary of this property is that, at this point of occurrence of flat contact $\mathcal{M} = (\hat{X}, \hat{Y}_p, \hat{L})$, there cannot exist other solutions such as a line contact solution or a flat contact solution with a

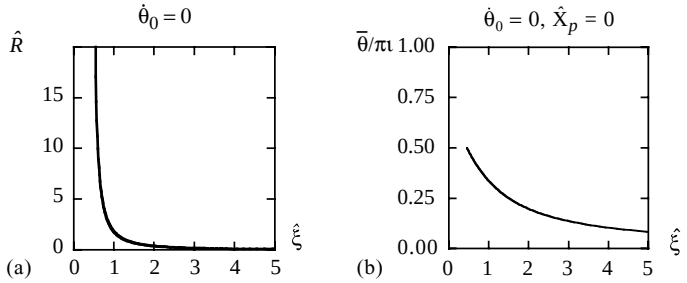

Fig. 9. Flat contact with vanishing length: $\dot\theta_0 = 0$, $\hat X_\mathrm{p} = 0$: (a) relative surface excess $\hat R$ vs. $\hat\xi$; (b) angle $\bar\theta/\pi$ vs. $\hat\xi$.

non-zero flat length $\hat X_\mathrm{p}$, since they would generate an additional flat contact occurrence at another height $\hat Y \neq \hat Y_\mathrm{p}$ by further increase or decrease of $\hat Y$.

4.2.3. *Fold uniqueness at flat contact occurrence*

At points $\mathcal{M}$, only flat contact solutions with vanishing flat length $\hat X_\mathrm{p}$ thus exist. Could they nevertheless correspond to different fold forms?

Following relations (A.5) and (A.6), fold constraints $(\hat X, \hat Y, \hat L)$ yield a *single* determination of $(\bar\theta, \omega)$ in the flat contact domain. This, from (A.1), implies a *unique* tension $\mathbf{T} = (p, q)$ and thus a *unique* Euler's equation (1) for this configuration. As initial conditions are prescribed by vanishing of both angle and angle derivative here, $(\theta_0, \dot\theta_0) = (0, 0)$, determinism of the Euler's equation then imposes a *single* fold form at points $\mathcal{M}$.

4.2.4. *Fold uniqueness in the flat contact domain*

Further compression from these states yields flat contacts to increase: $X_\mathrm{p} \neq 0$. Does fold uniqueness extend to these states?

Let us consider a sheet made of a fold of length $(\hat X, \hat Y, \hat L)$ prolongated by a flat contact of length $\hat X_\mathrm{p}$ (Fig. 1b). Let us label L its length and (X, Y) the dimensions of the box in which it is enclosed. We have $L = \hat L + \hat X_\mathrm{p}$, $X = \hat X + \hat X_\mathrm{p}$, $Y = \hat Y$. On the other hand, relations (A.6) state that $\tan\bar\theta = \hat Y/\hat X$ with $\bar\theta = \bar\Theta(\hat\xi)$ and $\hat\xi = \hat Y/(\hat L - \hat X)$. As $\hat\xi = Y/(L - X)$ and $\hat X_\mathrm{p} = X - Y/\tan\bar\theta$, the uniqueness of $\hat X_\mathrm{p}$ reduces to the uniqueness of $\bar\theta$ at given (X, Y, L) or, equivalently, to the bijective character of the function $\bar\Theta(\cdot)$. Fig. 9b reveals that this is actually the case: constraints (X, Y, L) impose a *single* $\hat X_\mathrm{p}$. Then, for given total lengths (X, Y, L), uniqueness of $\hat X_\mathrm{p}$ implies uniqueness of the dimensions $(\hat X, \hat Y, \hat L)$ of the remaining fold. As this fold involves by definition a vanishing flat contact length, its form is, following Section 4.2.3, univocally prescribed by its lengths. This demonstrates the *uniqueness* of fold form in the case of a flat part of *any* extent.

4.3. *Uniqueness for folds satisfying* $\hat X = 0$

We first use the variational character of the system to deduce a property of any couple of family of solutions joining two points where uniqueness is satisfied. We then apply this property to the line of states satisfying $\hat X = 0$. Notice that, as we shall not consider lateral box boundaries, no additional contact point will occur in between the compressing plates.

For fixed length $\hat L \equiv 1$, consider two states A, B, standing at different values of $(\hat X, \hat Y)$ and for which fold uniqueness is satisfied. Introduce a compression path $\mathcal{P}$ between A and B and assume that there exists at least two different branches of solutions $\mathcal{T}$, $\mathcal{T}'$ on that path. This allows one to make a cycle $\mathcal{C}$ starting from A, going to B

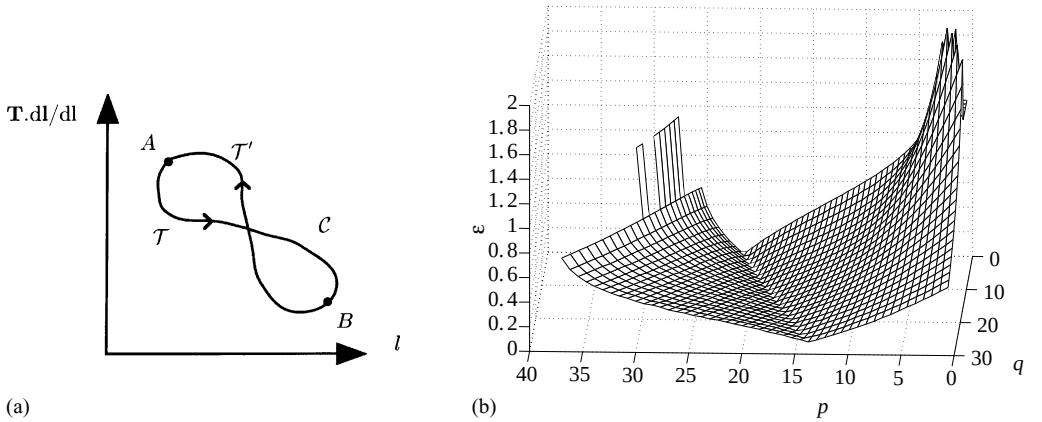

Fig. 10. (a) Cycle made on a given path $\mathcal{P}$ by going from A to B on one branch of solution, $\mathcal{T}$, and returning back to A on a second branch $\mathcal{T}'$. Graph shows, on each branch of solution, the gradient of work furnished by the operator, $\mathbf{T}\cdot\mathrm{d}\mathbf{l}/\mathrm{d}l$, where $\mathrm{d}\mathbf{l} = (\mathrm{d}\hat{X}, \mathrm{d}\hat{Y})$. Energy conservation asks for a net vanishing work on the cycle, therefore implying crossing of branches in this representation, i.e. $\delta\mathbf{T}\cdot\mathrm{d}\mathbf{l} = 0$ here. b) Error function $\epsilon(p, q_\mathrm{s})$ on the line $\hat{X} = 0$ when scanning for alternate solutions than the branch $(p_\mathrm{s}, q_\mathrm{s})$. This function can only vanish in a finite domain, on which it is actually scanned. It does so on a single line, however, therefore giving evidence of a *single* branch of solution.

on one branch of solution $\mathcal{T}$ and returning to A on the other branch of solution $\mathcal{T}'$ on the same path $\mathcal{P}$ in parameter space (Fig. 10a). Calling $\delta\mathbf{T} = (\delta p, \delta q)$ the variation of (p, q) between these two branches at given $(\hat{X}, \hat{Y})$, the work W made on the cycle $\mathcal{C} = \mathcal{T}\cup\mathcal{T}'$ writes

$$W = \oint_{\mathcal{C}} \mathbf{T}\cdot\mathrm{d}\mathbf{l} = \int_{\mathcal{T}} \delta\mathbf{T}\cdot\mathrm{d}\mathbf{l}, \tag{18}$$

where $\mathrm{d}\mathbf{l} = (\mathrm{d}\hat{X}, \mathrm{d}\hat{Y})$. However, by energy conservation (5), W also equals the difference of curvature energy E_c on the *closed* cycle $\mathcal{C}$, i.e. zero:

$$W = \Delta E_\mathrm{c} = 0. \tag{19}$$

Following this, the term $\delta\mathbf{T}\cdot\mathrm{d}\mathbf{l}$ must *vanish* at least *one time* on path $\mathcal{P}$.

On the line $\hat{X} = 0$, let us call P the state involving a flat contact with vanishing length and Q the unloaded state $q = 0$ (Fig. 12b). From Sections 4.1 and 4.2, we know that uniqueness of solutions is satisfied on both of them. Let us show that this property extends to the *whole* segment PQ by applying the above result to the straight path PQ.

For this, we first notice that, if two different solutions are found somewhere on path PQ, both of them nevertheless yield the same states at P and Q by increase or decrease of height $\hat{Y}$, thanks to fold uniqueness in the corresponding configurations (Sections 4.1 and 4.2). Accordingly, these solutions yield different branches of solutions connecting P to Q. However, on these paths, $\delta\mathbf{T}\cdot\mathrm{d}\mathbf{l} = \delta q\,\mathrm{d}\hat{Y}$ since PQ is parallel to the $\hat{Y}$-axis. Following (18) and (19), this implies that there *necessarily* exists at least *one* point C in between P and Q, where δq vanishes: the two branches of solution must *cross* in variable q.

At point C, the problem of uniqueness actually reduces to whether δp vanishes or not. Indeed, if $\delta p \neq 0$, solutions are different. On the opposite, if $\delta p = 0$, both p, q and thus the Euler's equation are the same for the two solutions. As their folds also correspond to the same constraints $(\hat{X}, \hat{Y}, \hat{L})$, they satisfy, from (3) and (9), the same initial conditions. They must therefore definitely be the *same*.

To test uniqueness at point C, we have performed numerical simulations of the Euler's equation on the line PQ, at *fixed* q and *variable* p. We have first determined a branch of solution going from P to Q that we label by index "s" below. Then, at given $\hat{Y}_\mathrm{s}$, q was fixed at the value q_s and p was varied. Initial impulsion was taken at the *only* value

capable of yielding, according to (9), both $\hat{X} = 0$ and $\hat{Y} = \hat{Y}_s$: $\dot{\theta}_0 = p\hat{Y}_s/2$. Denoting $(\hat{X}_a, \hat{Y}_a, \hat{L}_a)$ the lengths of this sole possible candidate, its relevance as a solution for constraints $(\hat{X}_s \equiv 0, \hat{Y}_s, \hat{L}_s)$ was detected as a zero of the error function $\epsilon^2(p, q_s) = (\hat{X}_a - \hat{X}_s)^2 + (\hat{Y}_a - \hat{Y}_s)^2 + (\hat{L}_a - \hat{L}_s)^2$. Fortunately, the range of p to be scanned is, at each point of the line *PQ*, *bounded*. This follows from the fact that, given $\dot{\theta}_0 = p\hat{Y}_s/2$ and $q \equiv q_s$, the relationship (8) is quadratic in p with *bounded* coefficients. It therefore constraints p to a *finite* range. Accordingly, seeking for an alternate solution at fixed q comes down to seeking for the zeros of function $\epsilon(p, q)$ in a *finite* domain. As shown in Fig. 10b, the result is a *convex* function $\epsilon(\cdot, \cdot)$ displaying a *single* line of zeros: $p = p_s$. There thus only exists a *single* solution at *fixed* q on the line $\hat{X} = 0$.

Following this result, on the line $\hat{X} = 0$, $\delta q = 0$ implies $\delta p = 0$, and thus, uniqueness. Thanks to this property, the same reasoning as above can be indefinitely *iterated* in between any couple of points satisfying uniqueness. It generates a point of uniqueness in between any other two and implies that, on the segment *PQ*, the set of points satisfying uniqueness is *dense*. By continuity, this set thus corresponds to this *whole* segment: uniqueness is satisfied on the line $\hat{X} = 0$.

4.4. Uniqueness in the domain of line contacts

We now turn our attention to the *whole constraint space* $\mathcal{S} = \{(\hat{X}, \hat{Y}), \hat{L} \equiv 1\}$. The previous results on uniqueness obtained in Sections 4.1–4.3 apply on three lines of $\mathcal{S}$ which form a *closed* contour surrounding the line contact domain (Fig. 12b). Our goal is to *extend* uniqueness from this frontier to the inner *domain* that it encloses.

We first notice that, within our definition of folds, curvature energy (11) is a function of $(p, q, \hat{X}, \hat{Y}, \hat{L})$ only. Assume now that there exists two branches of solution and consider the difference δE_c of their curvature energy at given $(\hat{X}, \hat{Y})$, $\hat{L} \equiv 1$. As the curvature energy E_c, the function δE_c is differentiable with respect to variables $(\hat{X}, \hat{Y})$. In particular, as tension $\mathbf{T} = (p, q)$ derives at fixed $\hat{L}$ from curvature energy by $\mathbf{T} = -\nabla_{\hat{X},\hat{Y}} E_c$ (5), the gradient of δE_c in the $(\hat{X}, \hat{Y})$ space simply stands as the difference between the tensions $\mathbf{T}$ on branches of solution:

$$\delta\mathbf{T} = (\delta p, \delta q) = \nabla_{\hat{X},\hat{Y}} \delta E_c. \tag{20}$$

Consider now, in the constraint space $(\hat{X}, \hat{Y})$, the function δE_c on a *closed* domain $\mathcal{D}$ on the frontier of which uniqueness, i.e. in particular $\delta E_c = 0$, is satisfied. If an extremum of δE_c is reached on the frontier of $\mathcal{D}$, it is thus by definition zero. If it is reached in the interior of $\mathcal{D}$, then $\nabla_{\hat{X},\hat{Y}} \delta E_c$ vanishes at this point. According to (20), this implies $\delta p = 0$, $\delta q = 0$ there and thus, from (11), $\delta E_c = 0$ too! (Fig. 11). In any case, the extrema of δE_c in $\mathcal{D}$ are zero. This implies that δE_c vanishes in the *whole* domain $\mathcal{D}$. Its gradient, i.e. $(\delta p, \delta q)$, therefore vanishes too, so that uniqueness is satisfied in $\mathcal{D}$. This result ensures uniqueness in the *whole* domain of line contact $\mathcal{L}$ (Fig. 12b).

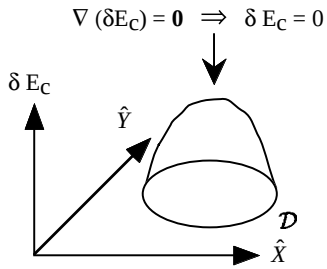

Fig. 11. Fundamental property of the difference of curvature energy δE_c between branches of solutions: it vanishes at its extrema. This implies that δE_c must be a *flat* surface, i.e. a zero-surface here: $\delta E_c = 0$.

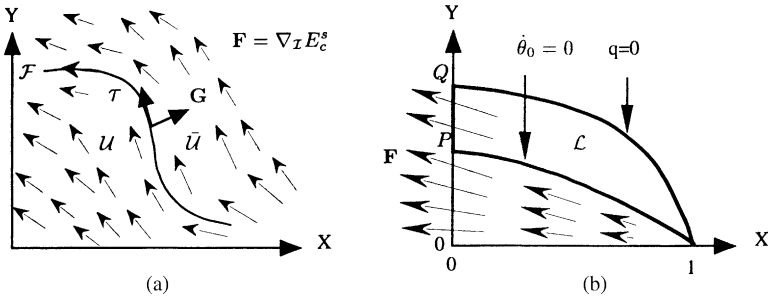

Fig. 12. Sketch of the flow of uniqueness $\mathbf{F} = \nabla_{\mathcal{I}} E_c^s|_{\mathcal{E}}$ in the constraint space of folds possibly prolongated by a flat part (Fig. 1a): (a) $\mathcal{F}$ denotes the frontier of the uniqueness domain $\mathcal{U}$, τ its tangent and $\mathbf{G} = \delta\mathcal{I}/|\delta\mathcal{I}|$ its normal. The flow $\mathbf{F}$ must be normal to $\mathbf{G}$ (28). In two dimensions, it must thus be tangent to frontier $\mathcal{F}$. (b) In the two-dimensional space $\{(X, Y, \theta_0 = 0), L \equiv 1\}$, the flow $\mathbf{F}$ propagates uniqueness away from domain $\mathcal{L}$.

4.5. *Flow of uniqueness in the fold space*

For completeness, we extend here the definition of folds so as to include a *single* extended flat contact, like the sheet forms displayed in Fig. 1c or half of Fig. 2a. Notice that this extended definition nevertheless excludes the juxtaposition of a fold with a free-standing fold and, therefore, the buckling of the added flat part. We label $(X, Y, L \equiv 1)$ the fold lengths and $\mathcal{S} = \{(X, Y), L \equiv 1\}$ its constraint space.

In $\mathcal{S}$, we consider the points where branches of fold solutions of the Elastica bifurcate. Our goal is to derive the conditions imposed at these bifurcation points by the structure of the Elastica. For this, we shall use the fact that Elastica's solutions satisfy an extremum principle (4) and that the Euler's model satisfies energy conservation (5) and (A.8). This will provide in Section 4.5.1 a general property of uniqueness domains that will be applied in Section 4.5.2 to fold uniqueness.

To address this problem in its full generality, we do not restrict ourselves to the clamping condition $\theta_0 = 0$. This will enable us to better emphasize the specific property of the present configuration in Section 4.5.2.

We label $\mathcal{I}$ the set of "intensive" variables $\mathcal{I} = (p, q, \dot{\theta}_0)$, $\mathcal{E}$ the set of "extensive" variables $\mathcal{E} = (X, Y, \theta_0)$ and we denote $d(\cdot)$ the variations between two folds satisfying the same constraints (X, Y), irrespective of whether they are Elastica solutions or not. However, in the case where both of them are Elastica solutions, we shall denote the variations between them with $\delta(\cdot)$. In the same spirit, curvature energy is denoted E_c, except for Elastica solutions for which a superscript "s", E_c^s, recalls that they refer to a steady state. Notice that, from (14), E_c^s expresses as a function of $\mathcal{I}$ and $\mathcal{E}$, $E_c^s \equiv E_c^s(\mathcal{I}, \mathcal{E})$, the variables $\mathcal{I}$ being definitely related to $\mathcal{E}$ on each branch of solution: $\mathcal{I} \equiv \mathcal{I}(\mathcal{E})$. Accordingly, on any *branch* of solution, E_c^s can be considered as a definite *function* of $\mathcal{E}$, $E_c^s \equiv E_c^s(\mathcal{E})$, this function changing from branch to branch, however.

4.5.1. *Property of the uniqueness domain*

In the space of extensive variables $\mathcal{V} = \{\mathcal{E}\} = \{(X, Y, \theta_0), L \equiv 1\}$, we consider the uniqueness domain $\mathcal{U}$ where constrained Elastica admits a single solution. Section 4.4 ensures that $\mathcal{U}$ is not empty, nor reduced to a point or a line. As $\mathcal{U}$ corresponds by definition to $\delta(\cdot) \equiv 0$, it is, by continuity, a *closed* set, i.e. a set which contains its own frontier $\mathcal{F}$. Our goal consists in determining some property of $\mathcal{F}$, i.e. in particular, a relationship for the directions τ of its tangent vectors (Fig. 12a).

We first notice that, *around* an Elastica solution, the variation of the curvature energy E_c with the sheet form satisfies, at *first* order in form variation, energy conservation (A.8) (see Appendix A.2):

$$\mathrm{d}E_c = -p\,\mathrm{d}X - q\,\mathrm{d}Y - \dot{\theta}_0\,\mathrm{d}\theta_0 = -\mathcal{I}\,\mathrm{d}\mathcal{E}. \tag{21}$$

Applying relation (21) on a given branch of solution, the gradient of curvature energy of Elastica *solutions* $E_c^s(\mathcal{E})$ with respect to extensive variables $\mathcal{E}$ reads

$$\nabla_{\mathcal{E}} E_c^s = -\mathcal{I}. \tag{22}$$

We stress that, in the non-uniqueness domain $\bar{\mathcal{U}}$, the vectors $\mathcal{I}$ related to different branches of solutions differ, $\delta\mathcal{I} \neq 0$, otherwise these branches would correspond to the same Euler equation $(\delta p, \delta q) = (0, 0)$, with the same initial conditions $(\delta\theta_0, \delta\dot{\theta}_0) = (0, 0)$, and thus to the same solution. Accordingly,

$$\delta\nabla_{\mathcal{E}} E_c^s = \nabla_{\mathcal{E}}\delta E_c^s = -\delta\mathcal{I} \neq 0 \quad \text{for } \mathcal{E} \in \bar{\mathcal{U}}. \tag{23}$$

In the non-uniqueness domain $\bar{\mathcal{U}}$, we now introduce the unit gradient $\mathbf{G}$:

$$\mathbf{G} = \frac{\nabla_{\mathcal{E}}(\delta E_c^s)}{|\nabla_{\mathcal{E}}(\delta E_c^s)|} = \frac{\delta\mathcal{I}}{|\delta\mathcal{I}|} \tag{24}$$

and we prolongate it by continuity on the frontier $\mathcal{F}$. However, as $\delta E_c^s = 0$ is satisfied *on* $\mathcal{F}$, this frontier is an iso-δE_c^s. Its direction is thus normal to $\mathbf{G}$ (Fig. 12a)

$$\tau \cdot \mathbf{G} = 0 \quad \text{for } \mathcal{E} \in \mathcal{F}. \tag{25}$$

Relation (25) provides a partial information on the direction of the frontier $\mathcal{F}$ and on the possible locations of a splitting of solutions. Our purpose is now to improve its characterization. For this, we notice that, following relation (21), the variation of curvature energy with sheet form at *fixed* extensive variables, i.e. $\mathrm{d}\mathcal{E} = 0$, is extremum *at* Elastica *solutions*:

$$\mathrm{d}\mathcal{E} = 0 \Rightarrow \mathrm{d}E_c = 0 \quad \text{around} \quad E_c \equiv E_c^s. \tag{26}$$

In particular, in the *vicinity* of bifurcation points, i.e. of the frontier $\mathcal{F}$, the difference between the curvature energy of two Elastica solutions referring to the *same* extensive variables $\mathcal{E}$ vanishes at *first* order in form variation: $\delta E_c^s = 0$. This information is interesting since the variation of δE_c^s between two Elastica solutions at *fixed* extensive variables $\mathcal{E}$ simply writes

$$\delta E_c^s = \nabla_{\mathcal{I}} E_c^s|_{\mathcal{E}} \cdot \delta\mathcal{I}, \tag{27}$$

where $\nabla_{\mathcal{I}} E_c^s|_{\mathcal{E}}$ denotes the gradient of curvature energy $E_c^s(\mathcal{I}, \mathcal{E})$ with respect to intensive variables $\mathcal{I}$ at *fixed* $\mathcal{E}$. Following (26) and (27), one thus obtains, in the vicinity of $\mathcal{F}$:

$$\nabla_{\mathcal{I}} E_c^s|_{\mathcal{E}} \cdot \frac{\delta\mathcal{I}}{|\delta\mathcal{I}|} \to 0 \quad \text{for} \quad \mathcal{E} \to \mathcal{F}, \quad \mathcal{E} \in \bar{\mathcal{U}}. \tag{28}$$

From the preceding relations, we can now derive a property of bifurcation points in the space of extensive variables $\mathcal{V}$.

According to (24), (25) and (28) the vectors $\nabla_{\mathcal{I}} E_c^s|_{\mathcal{E}}$ and τ are normal to the *same* vector $\mathbf{G} = \delta\mathcal{I}/|\delta\mathcal{I}|$ on the frontier $\mathcal{F}$. As the $\mathcal{V}$ space is three-dimensional, this can be written as

$$[\tau \wedge \nabla_{\mathcal{I}} E_c^s|_{\mathcal{E}}] \wedge \mathbf{G} = \mathbf{0} \quad \text{for} \quad \mathcal{E} \in \mathcal{F}. \tag{29}$$

Notice that, as relations (24) and (28) basically result from the extremum principle, they are only valid at the *first* order in form variation. For this reason, relation (29) is also valid at this order only. This relationship is nevertheless quite interesting here since it provides a property capable of discriminating the bifurcation points. In particular, any domain of uniqueness can be prolongated until this bifurcation requirement is satisfied. This property enables us to extend below the uniqueness domain found in Section 4.4.

4.5.2. Application to fold uniqueness

The property (29) contains information on the frontier $\mathcal{F}$ of the uniqueness domain $\mathcal{U}$. Our goal is now to exploit it to determine the locations of the bifurcations of branches of solutions in the present constrained Elastica problem.

On folds, either $\dot{\theta}_0 = 0$ or $\dot{\theta}_0 = (pY - qX)/2$ (9). As, in addition, θ_0 is fixed to 0 in our set-up, the above analysis can be reduced to the two-dimensional sets of variables $\mathcal{I} = (p, q)$ and $\mathcal{E} = (X, Y)$ here. Then, all vectors entering relation (29) are *two-dimensional*.

On the other hand, the analysis of the integral relationships of Elastica shows that form variation, e.g. $\delta\theta_\mathrm{I}$, and parameter variation $\delta\mathcal{I} = (\delta p, \delta q)$ are actually of the *same* order: $\delta\mathcal{I} = \mathrm{O}(\delta\theta_\mathrm{I})$ (see Appendix A.3). This ensures that relation (29) is *non-degenerate* here at the first order in form variation. Being relevant to vectors belonging to the *same* plane, this relation then states that the tangent vector τ and the flow $\mathbf{F} = \nabla_\mathcal{I} E_\mathrm{c}^\mathrm{s}|_\mathcal{E}$ are *parallel* on frontier $\mathcal{F}$ (Fig. 12a):

$$\tau \wedge \nabla_\mathcal{I} E_\mathrm{c}^\mathrm{s}|_\mathcal{E} = \mathbf{0} \quad \text{for} \quad \mathcal{E} \in \mathcal{F}. \tag{30}$$

Notice that, following (11), $\mathbf{F}$ reads for a line contact, i.e. for $\dot{\theta}_0 \neq 0$:

$$\mathbf{F} = \nabla_\mathcal{I} E_\mathrm{c}^\mathrm{s}|_\mathcal{E} \equiv \nabla_{(p,q)} E_\mathrm{c}^\mathrm{s}|_{(X,Y)} = \begin{vmatrix} -(L - X) + \frac{1}{4} YL(pY - qX) \\ Y - \frac{1}{4} XL(pY - qX) \end{vmatrix} \tag{31}$$

and for a planar contact, i.e. $\dot{\theta}_0 = 0$:

$$\mathbf{F} = \begin{vmatrix} -(L - X) \\ Y \end{vmatrix} \tag{32}$$

It should be emphasized that $\mathbf{F}$ cannot vanish here: $\mathbf{F} \neq \mathbf{0}$. In the planar contact regime, this follows from the fact that $\mathbf{F} = \mathbf{0}$ corresponds to $Y = 0$ and $L = X$, i.e. to the degenerate case of a flat sheet that is actually forbidden in the present constrained configuration. In the line contact domain, vanishing of $\mathbf{F}$ would require $Y^2 = X(L - X)$. However, at the occurrence of planar contacts, relations (9) and (11) imply that $E_\mathrm{c} = q[Y^2 - X(L - X)]/Y$ with positive q and E_c. Accordingly, Y^2 is larger than $X(L - X)$ at the occurrence of the planar contact regime and *a fortiori* in the line contact regime for which Y is even higher. Accordingly $\mathbf{F}$ cannot vanish.

Relation (30) means that frontier $\mathcal{F}$ can only be made of *streamlines* of the flow $\mathbf{F} = \nabla_\mathcal{I} E_\mathrm{c}^\mathrm{s}|_\mathcal{E}$. Reciprocally, as the simply connected parts of frontier $\mathcal{F}$ can only be a closed curve or an infinite curve, relation (30) implies that, if a streamline of $\mathbf{F} \neq \mathbf{0}$ contains a *single* point of uniqueness, it is *entirely* made of uniqueness points. The flow $\mathbf{F}$ therefore *transports* uniqueness within the constraint space $\mathcal{S} = \{(X, Y), L \equiv 1\}$. As a result, the uniqueness domain $\mathcal{U}$ is *invariant* by $\mathbf{F}$.

Following these properties, the domain of uniqueness $\mathcal{L}$ found in Section 4.4 may be viewed as a *source* of uniqueness that is spread by the flow $\nabla_{(p,q)} E_\mathrm{c}^\mathrm{s}|_{(X,Y)}$ in the constraint space of folds. It thus generates a larger uniqueness domain extending to the *whole* current tube crossing $\mathcal{L}$.

This property, which denies bifurcation between branches of solutions of a dynamical system in definite current tubes is, to our knowledge, original. We notice that it relies on quite general properties that could be encountered in many kinds of other dynamical systems: existence of a free energy E_c depending on few intensive parameters and continuous even at bifurcation. Interestingly, these criteria include second order thermodynamic phase transitions in confined systems.

The advection of uniqueness in the constraint space of folds may be illustrated in the particular case of planar contacts for which $\mathbf{F} = [-(L - X), Y]$. Here, $\mathbf{F}$ is a divergent flow whose streamlines are iso-ξ lines with $\xi = Y/(L - X)$. In the plane (X, Y), they form a set of radial lines emitted from the center $(X, Y) = (L, 0) \equiv (1, 0)$. In

agreement with the conclusion of Section 4.2.3, they then extend fold uniqueness from the domain $\mathcal{L}$ to the domain of planar contacts with a *non-zero* contact length $\hat{X}_p \neq 0$ (Figs. 1 and 12b), and even beyond.

5. Generalization and application to experiment

In previous sections, we have shown that there exists at most one unique *fold* with length $\hat{L}$ in a given box $(\hat{X}, \hat{Y})$. Here, we wish to address a similar issue in the more general configurations involved in experiment (Figs. 3–6): a *sheet* of length L enclosed in a box of sizes (X, Y). This leads us to address the following questions. How many sheet shapes can be observed in a given compressing box? Can the elastic response (p, q) of sheets take different values for the same imposed height? The property of fold uniqueness will be found essential to answer them.

Here, the main difference with the fold case is that sheets are usually made of a *juxtaposition* of several folds. Fold uniqueness already helps in addressing this more general situation properly since it denies the existence of different solutions if the corresponding length constraints $(\hat{X}, \hat{Y}, \hat{L})$ of their folds are the same. Accordingly, existence of multiple solutions for sheets compressed in a box can only be achieved by *differently* associating folds or by *varying* their length constraints.

Actually, it is well known from experiment [6–9] and simulations [4,10,11,16,18] that multiple solutions can be displayed when compressing a sheet into a box. Our goal here will then not be to prove multiplicity but rather to analyze and classify its different origins in this system. We shall find four of them: (i) gliding of contact points, (ii) rolling of contact points, (iii) flat part distribution and (iv) non-linearity.

The first two origins (i) and (ii) address a mean to generate asymmetry from the unique symmetric wrinkle that is found in the unloaded state at the beginning of compression routes (Section 4.1). Because of fold uniqueness, both ask for moving the contact point of sheets on the compressing plate so as to yield different geometrical constraints for the left fold and for the right fold. This may be obtained by gliding or by rolling, i.e. with or without friction. The third origin (iii) lies in an invariance of steady states with respect to flat part distributions. The last origin (iv) lies in geometrical non-linearity which provides an overlap of branches of solutions for free-standing folds.

5.1. Asymmetry with friction: gliding

We report here the main lines of a result which has pointed out the robustness of the Euler's model to friction [18]. Fold uniqueness was required to establish it, in anticipation to the demonstration of this property in the present work.

Addressing the occurrence of asymmetry with friction has been motivated by the striking observation following which, in our experiment, all the observed wrinkles satisfy a left–right symmetry whatever their history (Fig. 3), except when large amplitude external perturbations are involved (Fig. 6). This is somewhat surprising since this symmetry could be easily broken by friction at contact points, as different tensions p would then be generated on each fold. How can we then explain this large robustness of fold symmetry whereas no special care has been devoted to avoid friction?

The answer stands in a somewhat paradoxical role of friction which denies the spontaneous occurrence of the set of solutions that it nevertheless allows to exist. This may be understood by noticing that gliding of the sheet on the compressing plates at the contact points requires a sufficient amount of tension difference between the left fold and the right fold. However, prior to gliding, the geometrical constraints on these folds are the same. Thanks to *fold uniqueness*, they thus involve the *same* form and the *same* tension so that there is *no* tension difference at their contact point. Accordingly, the gliding threshold cannot neither be reached nor approached on the compression route, so that the wrinkle remains symmetric. This conclusion shows that symmetry and thus, a frictionless model

for sheet compression, is robust. In particular, asymmetry by gliding can only occur by finite amplitude perturbation generated by external mean (Fig. 6).

5.2. Asymmetry without friction: rolling

Another way to generate asymmetry from a symmetric wrinkle would be to let the contact point between sheet and plate roll. Then, no tension difference would occur on either sides of the contact point so that p would be the same on both of them. Analysis of the Elastica shows that there actually exists such asymmetric states made of two compressed sheets involving the same p, the same Y and the same curvature (i.e. the same $\dot\theta$) at their extremities [18]. Can they spontaneously occur on the compression route, however?

In the case of rolling of the contact point, the same length is transferred from the right fold to the left fold on the plate and on the sheet. Accordingly, the difference between L and X remains the same on both of them

$$\hat X \to \hat X + \epsilon\delta, \qquad \hat L \to \hat L + \epsilon\delta, \qquad \hat L - \hat X \to \hat L - \hat X, \tag{33}$$

where $\epsilon = 1$ on one fold and -1 on the other and where δ denotes the roll displacement. Thanks to *fold uniqueness*, we notice that, at the common contact point $C_\pm$ of these folds, both the tension p and the derivative $\dot\theta$ of the tangent angle to the sheet express as a *function* of the length constraints of the corresponding fold: $p \equiv p(\hat X, \hat Y, \hat L)$, $\dot\theta_{C_\pm} \equiv \dot\theta_{C_\pm}(\hat X, \hat Y, \hat L)$. Then, as curvature and tension p must be the same on both sides of the contact point, we obtain the following criterion for asymmetry:

$$p(\tfrac12 X + \delta, Y, \tfrac12 L + \delta) = p(\tfrac12 X - \delta, Y, \tfrac12 L - \delta)\dot\theta_{C+}(\tfrac12 X + \delta, Y, \tfrac12 L + \delta) = \dot\theta_{C-}(\tfrac12 X - \delta, Y, \tfrac12 L - \delta). \tag{34}$$

The spontaneous occurrence of asymmetry from the symmetric states, i.e. from $\delta = 0$, then both requires

$$\left(\frac{\partial p}{\partial X}\right)_{Y,L} + \left(\frac{\partial p}{\partial L}\right)_{X,Y} = 0, \qquad \left(\frac{\partial \dot\theta_C}{\partial X}\right)_{Y,L} + \left(\frac{\partial \dot\theta_C}{\partial L}\right)_{X,Y} = 0. \tag{35}$$

This restrictive criterion allows at most isolated bifurcation points. When they are not encountered or when the asymmetric branch is not taken there, asymmetry by rolling then requires large amplitude perturbation, as found in experiment (Fig. 6).

The above results show that the initial equality of the length constraints of folds in the unloaded sheets is robust at least in the line contact regime. This means that sheets that involve only two folds are simply equivalent to a couple of folds satisfying the same geometric constraints. Thanks to fold uniqueness, these folds are twins and their form is unique so that no multiple solutions can arise. Accordingly, we shall look hereafter for multiplicity in more complicated situations involving either free-standing folds or flat contacts.

5.3. Multiplicity in the flat contact regime: flat part distribution

Increasing compression from the unloaded state, all sheets necessarily develop a flat contact. This fact, which is well known from the experiment, has been demonstrated in Section 4.2.1. We show below that it provides the system with a new degree of freedom capable of generating multiplicity of solution.

As soon as a flat contact point appears, the sheet Hamiltonian (6) takes the value $H(\theta, \dot\theta) = -p$, since flatness at a contact point means $(\theta, \dot\theta) = (0, 0)$. As H is constant along the sheet (see Section 3.3), this implies that at *any* other contact point, the sheet involves a flat contact too: $(\theta = 0, H = -p) \Rightarrow \dot\theta = 0$. On a given sheet, contacts must therefore *all* be of the same kind.

Let us consider the occurrence of flat contacts, i.e. the states where their length X_p is zero. If the geometric constraints of folds are the same, then fold uniqueness states that these folds are the same. If they are not, the contact

point of the wrinkle with the compressing plate has either glided or rolled. We shall not consider the gliding case since, following Section 5.1, it requires finite amplitude perturbations and restrict our attention to the rolling case instead.

The rolling case involves no tension difference p between folds, no change of the length difference $\hat{L} - \hat{X}$ on each fold and thus the same value of $\hat{\xi} = \hat{Y}/(\hat{L} - \hat{X})$ for both folds. The bijective character of function $\bar{\Theta}(\cdot)$ (Fig. 9b) then implies that $\bar{\theta}$ is the same for both folds. Thanks to relations (A.1), tension component q is also the same on these folds. They thus involve the same tension and the same initial conditions $(\theta, \dot{\theta}) = (0, 0)$ at their contact point. By determinism of the Euler's equation, they are thus the same. This means that rolling cannot actually occur at the occurrence of flat contacts.

Further compression yields flat contact parts to extend, still by rolling: $X_\mathrm{p} \neq 0$. However, as flat parts correspond to rest states of the autonomous dynamical system that mimics the Euler's equation ($\dot{\theta}(s) = 0$), their *distribution* is obviously free (Fig. 5a), provided that their total length X_p gets the appropriate value required to satisfy the global constraints [14]. Here, the autonomy of the Euler's equation (Section 3.2), proves to be essential since the location of flat parts would not be arbitrary if the curvilinear abscissa appeared explicitly in it. However, given a solution displaying extended flat contacts, the arbitrary character of their distribution yields a continuous family of multiple solutions to be generated, simply by exchange of length from one plane contact to the other [14].

In particular, gathering all the flat contact length at a sheet extremity, we realize that determining the sheet form is a problem equivalent to that considered above for a zero flat contact length: $X_\mathrm{p} = 0$. Its conclusion is that, hereto, folds have the same shape and the same tensions. Moreover, distributing the contact length equally between the two folds yields a configuration similar to that addressed for a single fold with one plane contact (Section 4.2.3). Its conclusion states that their common shape and tension as well as the total contact length X_p are unique.

Changing the distribution of flat contacts yields configurations that involve the *same* folds and the *same* tension $\mathbf{T} = (p, q)$, but which are *not superposable*. However, their total curvature energy E_c is the same. In this sense they are equivalent from the point of view of elasticity. In particular, it costs no energy to move from one of these states to another so that, experimentally, one can change from one of these configurations to another by just applying a very small perturbation.

We do not consider this phenomenon as a real multiplicity. However, we will see later on that this neutral mode is related to the selection of multiple routes in the system.

5.4. Multiplicity in the free-standing fold regime: non-linearity

Sheets involving free-standing folds (Figs. 2b, 3c and 5b) are made of a juxtaposition of three folds: a left fold, a free-standing fold and a right fold. Even within a right-left symmetry, the existence of a free-standing fold provides a new degree of freedom for satisfying the global constraints. In particular, we already know two solutions satisfying constrained Elastica: one unstable (the sheet having not buckled) and one stable (the sheet having actually buckled).

We now restrict ourselves to examining the question of uniqueness *within* the family of sheets involving free-standing folds. One might first be tempted to simply generalize the derivation applied in Section 4.5.2 to folds. However, we show in Appendix A.4 that this could not work because, in the vicinity of the buckling bifurcation, a variation of form in this family drives a variation of intensive parameters at the *second* order only. This makes relation (29) *vanish* here at its relevant order, i.e. at the *first* order in form variation, so that it can no longer be used.

However, examining the vicinity of buckling from experiment and numerical simulation, we find evidence of a couple of solutions involving a free-standing fold for the same geometric constraints. This corresponds in Fig. 13

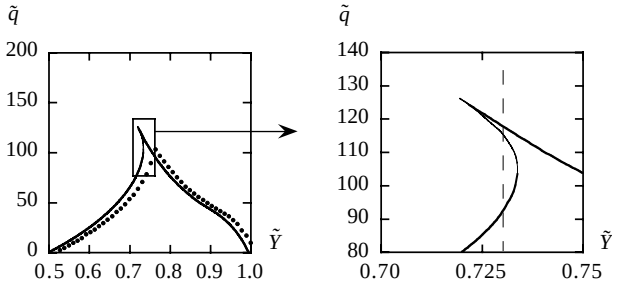

Fig. 13. Mechanical response of a sheet in non-dimensional variables $\tilde{q} = qL^2/EI$ vs. height $\tilde{Y} = Y/Y_1$. Here $Y_1 = 32.35\,\text{mm}$ is the height of unloaded fold (Fig. 3a), $I = h^3 l/12$, $E \approx 200\,\text{GPa}$, $h = 0.3\,\text{mm}$, $X = 220\,\text{mm}$, $L = 233\,\text{mm}$, $l = 101\,\text{mm}$, $R = 0.06$. Continuous line (resp. dotted line) corresponds to numerical integration of Euler's equation (resp. experiment). a) Force $\tilde{q}$ first increases as height is reduced. It undergoes buckling at the cusp point and then decreases on the free-standing fold branch (Fig. 3c) until eventually vanishing at $\tilde{Y} = 0.5$ when a free-standing fold generates two folds by touching the opposite plate (Fig. 3d). (b) Notice the multiplicity of numerical solutions in the range $0.719 < \tilde{Y} < 0.733$. It corresponds to a couple of different solutions at the *same* height $\tilde{Y}$, both involving a free-standing fold. The branch corresponding to $\mathrm{d}\tilde{q}/\mathrm{d}\tilde{Y} > 0$ (resp. < 0) is stable (resp. unstable).

to the couple of different states that stand at the same Y on the free-standing fold branch. The branch corresponding to $\mathrm{d}q/\mathrm{d}Y > 0$ is stable, but, following the exchange of stability at the connection between branches, the branch corresponding to $\mathrm{d}q/\mathrm{d}Y < 0$ is unstable. This exchange is also noticeable at the buckling bifurcation. The important thing, however, is the existence of a stable buckled branch below the onset of buckling. Following this, an additional unstable buckled branch is required to satisfy exchange of stability in this variational system.

As this multiplicity of solution is associated with different elastic responses, it may be considered as the first source of multiplicity found in this system. Its origin lies in the non-linearity of forms. However, as it involves only one stable branch of solution, it is not usually displayed in practice.

5.5. *Multiplicity of routes*

Another and more important source of multistability is related to the neutral mode that is generated by the freedom in distributing flat contact parts on a sheet (Fig. 5a).

It is well-known that the critical compression p_c at which a rod buckles depends on its length: the longer the rod, the smaller the critical load. However, on a given sheet, all flat contacts are subjected to the same force p so that the longer one will buckle the first. Following this, the distribution of planar parts drives important consequences for the sheet stability. At a given Y, a sheet will undergo buckling or not depending on the length of its *largest* planar domain: form multiplicity implies buckling multiplicity. In particular, the most unstable distribution corresponds to the total contact length concentrated on a single contact domain and the most stable repartition to this total contact length equally distributed on all the contact domains.

Due to this buckling multiplicity, the mechanical response of the system can differ from one experiment to the other since the distribution of plane contacts is sensitive to imperfections. This is in particular true for the emission of acoustic energy associated with buckling. More generally, it is remarkable that a neutral mode (regarding energy) proves to be of such a large importance for the evolution of this mechanical system.

Notice that this multistability is by no way in contradiction with fold uniqueness: form and tension of each fold are indeed *univocally* determined by fold lengths; however, there do exist *different* ways of associating several definite folds to satisfy the global sheet constraints (X, Y, L).

6. Conclusion

Constrained Elastica models the forms and tensions involved by sheets compressed within a box so as to display parallel folds. The compressing box introduces some bounds, the width X and height Y, to which the sheet of fixed length L has to adapt. We have investigated the uniqueness of the solutions to this boundary value problem by combining different complementary methods. They amount to determining whether the non-linear eigenvalues of the system (i.e. the tensions of the sheet here) are unique or multiple. The main problem was that solutions satisfying the same geometrical constraints (X, Y, L) might display forms *far distant* from each other, so that the search for uniqueness was actually a *non-local* quest regarding the sheet geometry.

We have first focussed attention on sheets involving a single contact with each of the compressing plates, the so-called folds. Here, the possibility of adding contact points is denied so that sheet geometry is the only degree of freedom left to adapt the box constraints. We have shown the uniqueness of solution in a number of special cases which form a closed path in the space of geometrical constraints $\mathcal{S} = \{(X, Y), L \equiv 1\}$, using exhaustive scans of the possible families of solutions and the formal elliptical integral solutions of the Elastica.

The goal was then to extend the property of uniqueness in the space $\mathcal{S}$. This was achieved first by using the fact that uniqueness was determined by the preceding method on a *closed* line in the space $\mathcal{S}$. In particular, the variational nature of the Elastica enabled us to extend uniqueness to the whole domain enclosed by that line, i.e. to the domain of line contacts. Finally, a dynamical vision of the uniqueness domain in parameter space has been deduced from considerations about the conditions for a splitting of branches of solutions. In particular, such bifurcation points could not occur on the streamline generated by a definite flow from any point where uniqueness was satisfied. This means that the uniqueness domain is stable by advection by this flow and, thus, that the property of uniqueness propagates itself in the space of geometrical constraints. Interestingly, this enabled us to extend it far away from the line contact domain.

To our knowledge, this is the first proof of uniqueness of solutions in constrained Elastica when the least number of contact points is allowed. We note that the strategy of this proof, which consists in extending uniqueness from definite states where it is simple to establish to a set of other states where direct proof is beyond actual capabilities, may be in principle applied to other dynamical systems involving a free energy.

Interestingly, this property of uniqueness can be used to save computational time in the numerical quest of solution and to detect parasitic solutions in numerical simulations [10,11]. Here, we also used it to establish the robustness of the Euler's model regarding friction by demonstrating that Elastica's solutions involving friction cannot spontaneously arise during crushing [18]. Finally, fold uniqueness has also been found essential to point out the different natures of the multiplicity of solutions that arise when other contact points than the sheet extremities are allowed: neutral mode for the distribution of flat parts in the flat contact regime; geometrical non-linearity in the buckled regime.

We have addressed a canonical issue in applied mathematics which, to our knowledge, had not previously been considered in constrained Elastica: the uniqueness of solutions in their most constrained configuration where only contact points at their extremities are allowed. Our proof includes a property that could be applied to other dynamical systems involving a free energy: the spreading of uniqueness by a definite flow in parameter space. Regarding elasticity, the uniqueness property provides useful information for simulations and for understanding the role of friction and the origin of multiplicity when additional contact points are allowed. More generally, the non-linear properties of compressed sheets that have been worked out here will worth being compared to those brought about by non-ideal compression systems (e.g. those involving some slight gradients), so as to emphasize the relevant mechanical differences implied by the inevitable imperfections of practical devices.

Appendix A

A.1. Formal solutions

We introduce

$$\tan\bar{\theta} = \frac{q}{p}, \qquad \omega^4 = \frac{p^2+q^2}{(EI)^2}, \quad q = EI\,\omega^2 \sin(\bar{\theta}), \quad p = EI\,\omega^2 \cos(\bar{\theta}) \tag{A.1}$$

and the elliptic integral of the first kind, $F(\phi, k)$, and of the second kind, $E(\phi, k)$:

$$F(\phi,k) = \int_0^{\phi} [1-k^2\sin^2(v)]^{-1/2}\,\mathrm{d}v, \qquad E(\phi,k) = \int_0^{\phi} [1-k^2\sin^2(v)]^{1/2}\,\mathrm{d}v \tag{A.2}$$

with

$$k = \sin\left(\frac{\theta_{\mathrm{I}}-\bar{\theta}}{2}\right), \qquad k\sin(\phi) = -\sin\left(\frac{\bar{\theta}}{2}\right) \tag{A.3}$$

the index I denoting the inflexion point of the sheet form: $\dot{\theta}_{\mathrm{I}} = 0$ (Fig. 7).

A.1.1. General solutions

Being analogous to a pendulum motion, the general solutions to constrained Elastica (1)–(3) can be expressed in terms of elliptic integrals:

$$\hat{X} = 2\int_0^{L/2} \cos(\theta)\,\mathrm{d}s = \frac{2}{\omega}(2\mathbf{E}-\mathbf{F})\cos(\bar{\theta}) - \frac{4}{\omega}k\cos(\phi)\sin(\bar{\theta}),$$
$$\hat{Y} = 2\int_0^{L/2} \sin(\theta)\,\mathrm{d}s = \frac{2}{\omega}(2\mathbf{E}-\mathbf{F})\sin(\bar{\theta}) + \frac{4}{\omega}k\cos(\phi)\cos(\bar{\theta}), \qquad \hat{L} = 2\int_0^{L/2}\mathrm{d}s = \frac{2\mathbf{F}}{\omega} \tag{A.4}$$

with $\mathbf{E} = E(\pi/2,k) - E(\phi,k)$ and $\mathbf{F} = F(\pi/2,k) - F(\phi,k)$. Here ϕ denotes the phase of the corresponding periodic orbit that is solution of the Euler's equation (1).

A.1.2. Flat contacts

In the case of planar contacts, i.e. $\dot{\theta}(0) = \dot{\theta}_0 = 0$, the relationships between lengths $(\hat{X}, \hat{Y}, \hat{L})$ and variables $(\bar{\theta}, k, \phi)$ look simplified

$$\hat{X} = \frac{4}{\omega}[2E-F](1-2k^2), \qquad \hat{Y} = \frac{4}{\omega}[2E-F]2k(1-k^2)^{1/2}, \qquad \hat{L} = \frac{4}{\omega}F \tag{A.5}$$

with $E = E(\pi/2,k)$, $F = F(\pi/2,k)$ and

$$k = \sin\left(\frac{\bar{\theta}}{2}\right), \qquad \phi = -\frac{\pi}{2}, \qquad \tan\bar{\theta} = \frac{\hat{Y}}{\hat{X}}, \tag{A.6}$$

where the latter relation follows from (9) and (A.1). Using these equations, one obtains an explicit link between the variables $\omega, k, \bar{\theta}$ and the ratios $\hat{\xi} = \hat{Y}/(\hat{L}-\hat{X})$ and $\hat{R} = \hat{L}/\hat{X} - 1$:

$$\hat{R} = F(k), \qquad \hat{\xi} = G(k), \qquad \omega = \frac{H(k)}{\hat{L}-\hat{X}}, \qquad \hat{R} = \hat{R}(\hat{\xi}), \qquad \bar{\theta} = \bar{\Theta}(\hat{\xi}), \tag{A.7}$$

where all functions are actually bijective (see Fig. 9 for functions $\hat{R}(\cdot)$ and $\bar{\Theta}(\cdot)$).

A.2. Energy conservation

The variation of curvature energy *around* an Elastica solution can be obtained from the Euler's equation

$$\delta E_c = \int_0^{\hat{L}} \delta[\tfrac{1}{2}\dot{\theta}^2]\,\mathrm{d}s = [\dot{\theta}\delta\theta]_0^{\hat{L}} - \int_0^{\hat{L}} \ddot{\theta}\delta\theta\,\mathrm{d}s = \int_0^{\hat{L}} [p\sin(\theta) - q\cos(\theta)]\delta\theta\,\mathrm{d}s - \dot{\theta}_0\delta\theta_0$$
$$= -p\delta\hat{X} - q\delta\hat{Y} - \dot{\theta}_0\delta\theta_0. \tag{A.8}$$

This relation generalizes energy conservation (5) to variations of initial angle θ_0.

A.3. Fold domain: order of variation of tension with form

In the fold domain, differentiation of relations (8) and (9) between two Elastica solutions yields

$$\delta p[\tfrac{1}{2}\hat{Y}\dot{\theta}_0 - 2\sin^2(\tfrac{1}{2}\theta_I)] + \delta q[\sin(\theta_I) - \tfrac{1}{2}\hat{X}\dot{\theta}_0] = EI\,\omega^2 \sin(\theta_I - \bar{\theta})\delta\theta_I, \tag{A.9}$$

where, in contrast with (8), the factor EI has been made explicit here.

The right-hand side of (A.9) only vanishes when $\theta_I - \bar{\theta} = 0$ or π, i.e. when $k = 0$ or 1 (A.3). However, relations (7), (A.1) and (A.3) show that $H = -\omega^2(1 - 2k^2)$. The case $k = 0$ therefore corresponds to the lowest possible value of the Hamiltonian H, for which there is no motion: $\theta \equiv 0$. The case $k = 1$ means that the pendulum motion described by the Elastica stands on the separatrix, so that an infinite time, i.e. an infinite length $\hat{L}$, is required to reach the inflexion point. As both these states conflict with the imposed constraints, they can be ignored here. We are thus left with cases for which the term $\sin(\theta_I - \bar{\theta})$ does not vanish. Then, relation (A.9) shows that form variation, e.g. $\delta\theta_I$, and parameter variation $\delta\mathcal{I} = (\delta p, \delta q)$ are actually of the *same* order: $\delta\mathcal{I} = \mathrm{O}(\delta\theta_I)$. This ensures that relation (29) is *non-degenerate* here at the first order in form variation.

A.4. Buckling bifurcation

We consider the buckling bifurcation following which a sheet involving flat contact parts generates a free-standing fold. We address the issue as to whether the derivation of fold uniqueness can be generalized to such configuration. We restrict analysis to right-left symmetrical sheets.

We first notice that, compared to folds, an additional degree of freedom is in order for sheets involving free-standing fold: the lateral extent $\hat{X}$ of the box in which the left fold is enclosed. This makes the initial impulsion $\dot{\theta}_0$ a free variable, no longer prescribed by the constraints (p, q, X, Y) only: $\dot{\theta}_0 = (p\hat{Y} - q\hat{X})/2$. Following this, relation (29) gets three-dimensional, instead of two-dimensional otherwise.

More importantly, we stress that, even if the analysis was extended to derive the implications of relation (29), it would not enable us to draw conclusions regarding uniqueness here. The reason is that, at the occurrence of a free-standing fold, the intensive variables (p, q) vary at *second* order with respect to form variation, so that the first-order relations (24) and (28) give actually no information.

Derivation of the order of variation of intensive variables with respect to the sheet's form is obtained by linearizing the Elastica in the vicinity of the buckling bifurcation, thanks to the nearly flat shape of the free-standing folds. This yields a straightforward computation of the difference $(\hat{L}_f - \hat{X}_f)$ of lengths relative to the free-standing folds, $(\hat{L}_f - \hat{X}_f) = \pi/4p^{1/2}\hat{Y}_f^2$, and implies that the difference $(\hat{L} - \hat{X})$ relative to each of the two remaining folds satisfies: $(\hat{L} - \hat{X}) = (L - X)/2 - \pi/8p^{1/2}\hat{Y}_f^2$ (Fig. 2b).

Our goal is now to compare the tension of the free-standing fold to that undergone by the sheet having not yet buckled. This is a priori an uneasy task since the former form involves line contacts whereas the latter form still

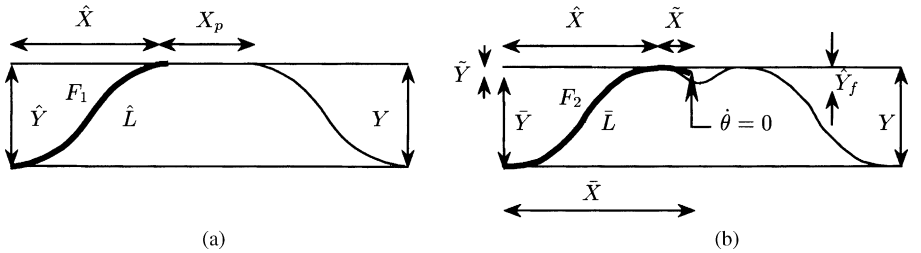

Fig. 14. Sketch of the real (but unstable) fold F_1 and of the virtual *prolongated* fold F_2. Both are shown with heavy lines: (a) the unstable fold F_1; (b) the prolongated fold F_2 ending at an inflexion point ($\dot{\theta} = 0$).

involves planar ones. To help comparing sheet tensions on the same basis, we then virtually prolongate the fold at the left of the free-standing fold until it displays an inflexion point mimicking a planar contact: $\dot{\theta} = 0$ (Fig. 14b). As this virtual prolongation involves no external action, sheet tension is actually conserved. One then obtains two folds both involving planar contacts: the real (but unstable) one F_1 to which we want to compare (Fig. 14a); the virtual (prolongated) one F_2 that refers to the buckled sheet (Fig. 14b).

Let us call $(\tilde{X}, \tilde{Y}, \tilde{L})$ the lengths relative to the additional part of the prolongated free-standing fold (Fig. 14b). Relation (6) shows that, for this fold, the angle θ decreases down to $\theta_\mathrm{f} = -\dot{\theta}_0^2/q$. Computation of the difference $(\tilde{L} - \tilde{X})$ brought about by this extension then yields

$$\tilde{L} - \tilde{X} = \int_0^{\theta_\mathrm{f}} \frac{1 - \cos(\theta)}{\dot{\theta}} \,\mathrm{d}\theta \approx \hat{Y}_\mathrm{f}^5 q^2 \left(\frac{p}{q}\right)^5 \tag{A.10}$$

since $\dot{\theta}^2 \approx q(\theta - \theta_\mathrm{f})$ and $\dot{\theta}_0 = p\hat{Y}_\mathrm{f}$ from (6). The total lengths $(\bar{X}, \bar{L})$ of the prolongated free-standing fold F_2 then satisfy

$$\bar{L} - \bar{X} = (\tilde{L} - \tilde{X}) + (\hat{L} - \hat{X}) = \frac{L - X}{2} - \frac{\pi}{8} p^{1/2} \hat{Y}_\mathrm{f}^2 + p^{1/2} \hat{Y}_\mathrm{f}^2 \mathrm{O}\left[(p^{1/2}\hat{Y}_\mathrm{f})^3 \left(\frac{p}{q}\right)^3 \right]. \tag{A.11}$$

In the same way, the height difference $Y - \bar{Y} = \tilde{Y}$ between the two folds F_1 and F_2 write

$$Y - \bar{Y} = \int_0^{\theta_\mathrm{f}} \frac{\sin(\theta)}{\dot{\theta}} \,\mathrm{d}\theta \approx \hat{Y}_\mathrm{f}^3 \frac{p^3}{q^2}. \tag{A.12}$$

To compare the tensions (p, q) of the folds F_1, F_2, we now recall that, in the case of flat contacts, they are functions of a single variable $\xi = Y/(L - X)$ (Section A.1.2). Here, this variable reads $\xi_2 = \bar{Y}/(\bar{L} - \bar{X})$ (resp. $\xi_1 = \hat{Y}/(\hat{L} - \hat{X})$) for fold F_2 (resp. F_1). Then, following (A.11), the difference $\delta\xi = \xi_2 - \xi_1$ is of *second order* with respect to the height $\hat{Y}_\mathrm{f}$ of the free-standing fold. This means that the differences $(\delta p, \delta q)$ between the tensions of these solutions are of *second order* too: $(\delta p, \delta q) = \mathrm{O}(\hat{Y}_\mathrm{f}^2)$. Accordingly, relation (29) identically vanishes at first order in form variation. The buckling bifurcation is thus too smooth compared to the information conveyed by the action principle to make it help characterizing the bifurcation points. Contrary to folds, relation (29) then fails to prescribe uniqueness, in agreement with counter-examples found from numerical simulations (Section 5.4 and Fig. 13b).

References

[1] L. Euler, Methodus inveniendi lineas curvas maximi minimive proprietate gaudentes, 1744.
[2] L.D. Landau, E.M. Lifschitz, Theory of Elasticity, Pergamon Press, New York, 1964.

[3] A. Pippard, The elastic arch and its modes of instability, Eur. J. Phys. 11 (1990) 359–365.
[4] P. Patricio, M. Adda-Beddia, M. Ben Amar, An elastica problem: instabilities of an elastic arch, Physica D 124 (1998) 285–295.
[5] G. Arreaga, R. Capovilla, C. Chryssomalakos, J. Guven, Phys. Rev. E 65 (2002) 031801, 1–13.
[6] A. Daubrée, Etudes synthétiques de géologie expérimentale, Dunod Editeur, Paris, 1879, pp. 288–300.
[7] H. Chai, The post-buckling response of a bi-laterally constrained column, J. Mech. Phys. Solids 46 (7) (1998) 1155–1181.
[8] H. Iseki, R. Sowerby, D. Bhattacharyya, P. Gatt, J. Appl. Mech. 56 (1989) 96–104.
[9] X. Chateau, Q.S. Nguyen, Buckling of elastic structures in unilateral contact with or without friction, Eur. J. Mech. A: Solids 10 (1) (1991) 71–89.
[10] G. Domokos, P. Holmes, B. Royce, Constrained Euler buckling, J. Nonlinear Sci. 7 (1997) 281–314.
[11] P. Holmes, G. Domokos, J. Schmitt, I. Szeberényi, Constrained Euler buckling: an interplay of computation and analysis, Comput. Meth. Appl. Mech. Eng. 170 (1999) 175–207.
[12] R. Plaut, S. Suherman, D. Dillard, B. Williams, L. Watson, Deflections and buckling of a bent elastica in contact with a flat surface, Int. J. Solids Struct. 36 (1999) 1209–1229.
[13] H. Paap, L. Kramer, Wavenumber restriction in systems with discontinuous nonlinearities and the buckling instability of plates, J. Phys. 48 (1987) 1471–1478.
[14] B. Roman, A. Pocheau, Buckling cascade of thin plates: forms, constraints and similarity, Europhys. Lett. 46 (5) (1999) 602–608.
[15] M. Boucif, J.E. Weisfreid, E. Guyon, Experimental study of wavelength selection in the elastic buckling instability of thin plates, Eur. J. Mech. A: Solids 10 (6) (1991) 641–661.
[16] G. Domokos, P. Holmes, Euler's problem, Euler's method, and the standard map; or, the discrete charm of buckling, J. Nonlinear Sci. 3 (1993) 109–151.
[17] H. Link, Uber den geraden Knickstab mit begrenzter Durchbiegung, Ing. Arch. 22 (1954) 237–250.
[18] B. Roman, A. Pocheau, Postbuckling of bilaterally constrained rectangular thin plates, J. Mech. Phys. Sol. 50 (2002) 2379–2401.
[19] S. Chucheepsakul, C.M. Wang, X.Q. He, T. Monprapussorn, J. Appl. Mech. 66 (1999) 87–94.
[20] A.E.H. Love, A Treatise on the Mathematical Theory of Elasticity, Cambridge University Press, Cambridge, UK, 1927.
[21] G.I. Barenblatt, Scaling, Self-similarity and Intermediate Asymptotics, Cambridge University Press, Cambridge, 1996.